

AD-A198 513

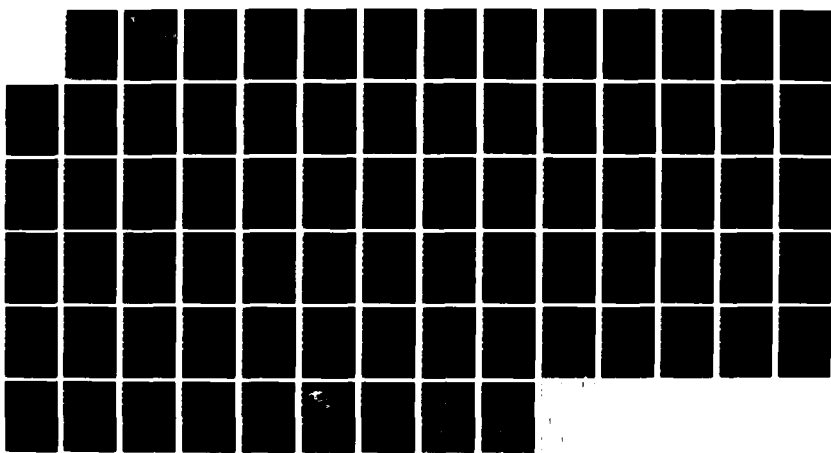
MPD (MAGNETOPLASMA DYNAMIC) THRUSTER ADVANCED PUMPING
SYSTEM CONCEPTS(U) ARGONNE NATIONAL LAB IL
S K BHATTACHARYYA ET AL DEC 87 AFAL-TR-87-067

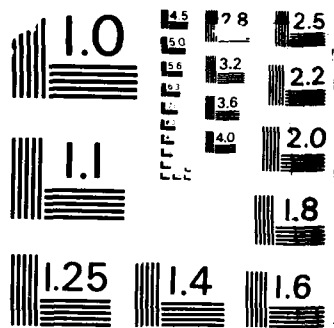
1/1

UNCLASSIFIED

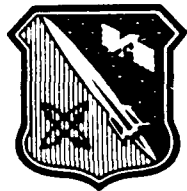
F/G 21/3

NL





MICROCOPY RESOLUTION TEST CHART
NATIONAL BUREAU OF STANDARDS-1963-A



AFAL-TR-87-067

AD:

AD-A190 513

Final Report
for the period
June 1985 to
August 1986

MPD Thruster Advanced Pumping System Concepts

DTIC
ELECTE
MAR 03 1988
S D

December 1987

Authors:
S. K. Bhattacharyya
L. W. Carlson
L. S. Chow
E. D. Doss
H. Herman
C. B. Reed

Argonne National Laboratory
9700 South Cass Ave.
Argonne, IL 60439

Order Number RPL 69005

Approved for Public Release

Distribution is unlimited. The AFAL Technical Services Office has reviewed this report, and it is releasable to the National Technical Information Service, where it will be available to the general public, including foreign nationals.

prepared for the:

**Air Force
Astronautics
Laboratory**

Air Force Space Technology Center
Space Division, Air Force Systems Command
Edwards Air Force Base,
California 93523-5000

88 3 04 048

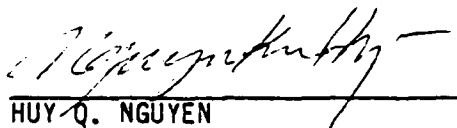
NOTICE

When U.S. Government drawings, specifications, or other data are used for any purpose other than a definitely related Government procurement operation, the fact that the Government may have formulated, furnished, or in any way supplied the said drawings, specifications, or other data, is not to be regarded by implication or otherwise, or in any way licensing the holder or any other person or corporation, or conveying any rights or permission to manufacture, use, or sell any patented invention that may be related thereto.

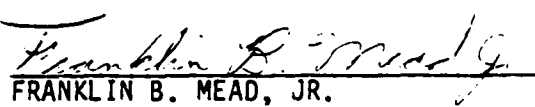
FOREWORD

This final report on MPD Thruster Advanced Pumping System Concepts was submitted by Argonne National Laboratory on completion of funding identification number RPL 69005 with the Air Force Astronautics Laboratory (AFAL), Edwards Air Force Base, CA. AFAL Project Manager was Capt Orin Kilgore, succeeded by Huy Q. (Tony) Nguyen.

This report has been reviewed and is approved for release and distribution in accordance with the distribution statement on the cover and on the DD Form 1473.

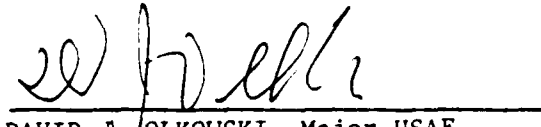


HUY Q. NGUYEN
Project Manager



FRANKLIN B. MEAD, JR.
Acting Chief, Advanced Propulsion
Branch

FOR THE COMMANDER



DAVID J. JOLKOWSKI, Major USAF
Deputy Chief, Liquid Rocket Division

REPORT DOCUMENTATION PAGE

Form Approved
OMB No. 0704-0188

1a. REPORT SECURITY CLASSIFICATION UNCLASSIFIED		1b. RESTRICTIVE MARKINGS AD - A190 513	
2a. SECURITY CLASSIFICATION AUTHORITY		3. DISTRIBUTION/AVAILABILITY OF REPORT Approved for public release; distribution is unlimited.	
2b. DECLASSIFICATION/DOWNGRADING SCHEDULE		4. PERFORMING ORGANIZATION REPORT NUMBER(S)	
4. PERFORMING ORGANIZATION REPORT NUMBER(S)		5. MONITORING ORGANIZATION REPORT NUMBER(S) AFAL-TR-87-067	
6a. NAME OF PERFORMING ORGANIZATION Argonne National Laboratory	6b. OFFICE SYMBOL (if applicable)	7a. NAME OF MONITORING ORGANIZATION Air Force Astronautics Laboratory	
6c. ADDRESS (City, State, and ZIP Code) 9700 South Cass Ave. Argonne, IL 60439		7b. ADDRESS (City, State, and ZIP Code) AFAL/LKCL Edwards AFB CA 93523-5000	
8a. NAME OF FUNDING/SPONSORING ORGANIZATION	8b. OFFICE SYMBOL (if applicable)	9. PROCUREMENT INSTRUMENT IDENTIFICATION NUMBER Order Number RPL 69005	
8c. ADDRESS (City, State, and ZIP Code)		10. SOURCE OF FUNDING NUMBERS	
		PROGRAM ELEMENT NO. 62302F	PROJECT NO. 5730
		TASK NO. 00	WORK UNIT ACCESSION NO. SE
11. TITLE (Include Security Classification) MPD Thruster Advanced Pumping System Concepts (U)			
12. PERSONAL AUTHOR(S) Bhattacharyya, S.K., Carlson, L.W., Chow, L.S., Doss, E.D., Herman, H., and Reed, C.B.			
13a. TYPE OF REPORT Final	13b. TIME COVERED FROM <u>85/6</u> TO <u>86/8</u>	14. DATE OF REPORT (Year, Month, Day) 87/12	15. PAGE COUNT 73
16. SUPPLEMENTARY NOTATION			
17. COSATI CODES		18. SUBJECT TERMS (Continue on reverse if necessary and identify by block number)	
FIELD 14	GROUP 02	Electric Propulsion, MPD Thrusters, Test Facilities, Pumping Systems.	
19. ABSTRACT (Continue on reverse if necessary and identify by block number)			
<p>Magnetoplasmadynamic (MPD) thrusters have a number of features that make them attractive for use in several intermediate term missions planned by the U.S. Air Force and NASA. Theoretical studies and laboratory scale pulsed tests performed to date have established the basic characteristics of MPD thrusters and have provided a basis for optimism regarding their eventual performance. The high (multimegawatt) power sources for space use currently being developed in the Strategic Defense Initiative can be adapted for use with MPD thrusters. Given these conditions, a major requirement for MPD thruster development is the availability of a suitable prototype test facility since successful development of multimegawatt MPD thrusters will depend, to a great extent, on testing them under realistic steady state space simulation conditions. Steady state testing is required to evaluate thermal characteristics, life cycle expectancy, electrode erosion rates, and other data essential to the design of working thrusters. The major technical obstacle for ground-</p>			
20. DISTRIBUTION/AVAILABILITY OF ABSTRACT <input type="checkbox"/> UNCLASSIFIED/UNLIMITED <input checked="" type="checkbox"/> SAME AS RPT <input type="checkbox"/> DTIC USERS		21. ABSTRACT SECURITY CLASSIFICATION UNCLASSIFIED	
22a. NAME OF RESPONSIBLE INDIVIDUAL HUY Q. (TONY) NGUYEN		22b. TELEPHONE (Include Area Code) (805) 275-5473	22c. OFFICE SYMBOL LKCL

testing of MPD thrusters in a space simulation facility is the inability of state-of-the-art vacuum systems to provide the tremendous pumping speeds that are required for multimegawatt MPD thrusters. This is true for other types of electric propulsion devices as well. This report discusses the efforts of a first phase or an evaluation of steady state MPD thruster test facilities and addresses the conceptual design of vacuum systems that are required to support testing of multimegawatt devices. Three advanced vacuum pumping concepts for this application were evaluated and are reported herein.

DTIC
COPY
INSPECTED
1

Accession For	
NTIS CRA&I	<input checked="" type="checkbox"/>
DTIC TAB	<input type="checkbox"/>
Unannounced	<input type="checkbox"/>
Justification	
By	
Distribution/	
Availability Codes	
Dist	Avail and/or Special
A-1	

Table of Contents

	<u>Page</u>
INTRODUCTION	1
Background	1
Statement of Work	3
Delivery Schedule	4
SYSTEMS REVIEWED	5
Conventional Pumping Systems	5
Vacuum System Considerations	7
PROPOSED ADVANCED PUMPING SYSTEMS	9
Argon Prebooster/Oil Vapor Booster Combination	9
Continuous Cryopumping System	11
Axisymmetric Linear Induction Plasma Pump (ALIPP)	13
Gasdynamic Diffuser/Enthalpy Extractor	16
COSTS	18
Common Costs	18
Argon Prebooster/Oil Vapor Booster System	19
Continuous Cryogenic System	20
ALIPP System	21
Summary of Cost Analyses	21
RATIONALE FOR PHASE II TEST PROGRAM	22
SUMMARY AND CONCLUSIONS	23
REFERENCES	24
APPENDIX: Design Calculations for Argon Prebooster System	

List of Tables

<u>No.</u>	<u>Title</u>	<u>Page</u>
1.	Large Vacuum Facility Characteristics	26
2.	Diffusion of Pumps	27
3.	Summary of Pumping Concept Features	28
4.	Argon Prebooster Enhanced Vacuum System Stage Conditions	29
5.	Summary of Advanced Pumping System Costs	30

List of Figures

1.	Stuttgart Facility Vacuum Capability	31
2.	Diffusion Pump Operating Regime	32
3.	Typical Pumping Characteristic Curves for Turbomolecular Pump	33
4.	Typical Pressures vs Steam-to-gas Mass Flow Ratios for Steam Ejectors	34
5.	Oil Vapor Booster Pump with Typical Characteristic Curve	35
6.	Argon Prebooster Block Diagram	36
7.	Oil Vapor Booster Pumping System Arrangement	37
8.	Operating Curves of Steady State Facilities	38
9.	Argon Prebooster Fitted to Vacuum Chamber	39
10.	Conventional Cryopumping Arrangement	40
11.	Continuous Cryopumping System with Mechanical Scraper	41
12.	Continuous Cryopumping System with Thermal Scraper	42
13.	Thermal Scraper Cross-section	43
14.	Axisymmetric Linear Induction Plasma Pump (ALIPP)	44
15.	Operating Principle of Axisymmetric Linear Induction Plasma Pump (ALIPP)	45
16.	Conductivity of Argon	46
17.	ALIPP Skin Depth	47
18.	MPD Thruster Vacuum System with Internal Cooling Diffuser . . .	48

INTRODUCTION

BACKGROUND

Magnetoplasmadynamic (MPD) thrusters are relatively low thrust (tens of newtons force), high specific impulse (several thousand seconds), space propulsion devices which require large amounts of electric power (multimegawatt) for optimum operation. MPD thrusters will be used in a variety of space missions wherein large velocity differentials will be required under low acceleration conditions. Thus, the MPD thrusters will be required to operate in a steady state condition for long periods of time (days) within the space vacuum (pressure $<10^{-10}$ torr) environment. This combination of operating conditions imposes severe problems in MPD thruster hardware design. The nature of these design problems is such that design margins are small and hardware must be thoroughly tested to insure that it will function properly under intended usage conditions. For example, wear-out characteristics of electrodes at the high current densities, high surface temperatures, and high heat fluxes must be determined in development tests conducted prior to mission use. It is known that electrode wear is a strong function of background pressure level, if this pressure is above 10^{-4} torr. These development tests could be conducted either in space or in an earth-based high vacuum facility. Though space testing would provide the ideal environment for thruster development in terms of (1) determining the effects of background pressure on electrode wear-out rates, (2) determination of plume expansion characteristics, and (3) evaluation of thruster performance, large electric power levels will not be available in space within the required development program time envelope. Also, space testing would be very inflexible and costly. In particular, experimental studies of several potential thruster designs will certainly be precluded. Ground testing is the only feasible alternative, even though no currently available ground-based vacuum facility can meet the simultaneous requirements of moderate vacuum (pressure $<10^{-4}$ torr) and relatively high propellant mass flow rate (approximately 6 g/s).

As previously stated, there is no currently available facility which can meet the simultaneous requirements of an MPD thruster electrode life test program (pressure $<10^{-4}$ torr, a flowrate of 6 g/s, and electrical power dissipation of several megawatts). The traditional method of testing MPD thrusters in ground-based vacuum facilities is to use a pulsed mode of operation (Refs. 1-5). Required flow rates are established for only milliseconds duration, with flows overlapping electric power pulses to the electrodes. Fast response instrumentation measures thrust and power transients and transient plume characteristics; specific impulse and power conversion efficiency are evaluated from these transient data. The vacuum systems have sufficient volume that the short duration flows do not raise the internal pressure above that which would compromise test data. While these tests have provided a wealth of basic data, they are unable to provide information on a number of critical MPD thruster performance features. For example, these tests do not allow for determination

of thruster wear-out rates because too many tests would be required over too long a test program duration. Also, it has been established by some investigators (Refs. 6 and 7) that the background pressure level has a large effect upon electrode wear rate for pressure levels above 10^{-4} torr. The current pulsed-operation tests need to be extended to more prototypic operating conditions. Accordingly, steady state ground tests at appropriate operating pressure levels ($<10^{-4}$ torr) are required to establish realistic MPD thruster operating parameters in a real space environment.

The steady state test conditions of pressure $<10^{-4}$ torr, temperature near ambient (300 K), and mass flow rate of 6 g/s represent a volumetric rate of approximately 4×10^7 liters per second. A literature search by the U.S. Air Force has determined the steady state capabilities of existing vacuum facilities in the "free world" (Ref. 8). The operating parameters of some of the larger of these facilities, which are located within the continental United States, are listed in Table 1. Most of these vacuum systems employ oil-type diffusion pumps. Some also incorporate cryogenically cooled (4 to 20 K helium) surfaces for added pumping capacity. Though some of these vacuum systems are not in use and have large internal free volumes (e.g., up to 100 ft dia by 122 ft height), none have sufficient flow or heat removal rate capacity. The largest systems might accommodate flows to 1/4 g/s and heat loads to a few hundred kilowatts.

The Air Force has used a vacuum facility which is located at the University of Stuttgart in West Germany for space simulation testing of MPD thrusters (Ref. 9). This facility has a volumetric flowrate capability of approximately 4,000 l/s at a pressure level of 10^{-4} torr. Thus, it falls short of the pumping rate requirement by a large margin. The vacuum pumping capacity curve at the Stuttgart facility is shown in Figure 1.

Argonne National Laboratory (ANL) was given a contract by the U.S. Air Force to assess the feasibility of designing a moderate vacuum (approximately 10^{-2} torr) space simulation MPD thruster test facility suitable for steady state operation and life testing of MPD thrusters at several megawatt power levels and at flow rates of argon gas up to 6 g/s. (The vacuum requirement was later increased to 10^{-4} torr.) Toward this objective, a number of commercial vacuum system vendors were approached to determine the present status of pumping systems. These included (1) Leybold-Heraeus, (2) Dresser Industries, (3) Consolidated Vacuum Corp. (CVC), (4) Edwards High Vacuum, (5) Stokes, (6) Kinney, (7) Fuller Corp. (Sutorbilt), (8) Corona Pumps, (9) Varian, (10) Balzers, and (11) Croll-Reynolds. These companies' products cover a wide variety of vacuum pumping systems based upon the following: Roots type blowers, mechanical type roughing pumps, steam ejectors, oil vapor diffusion pumps, oil vapor booster pumps, turbomolecular vacuum pumps, cryogenic pumps, ion pumps, and liquid ring pumps.

A discussion of the capabilities of the various types of vacuum pumping systems is presented later in this report, based upon literature supplied by

these various manufacturers and based upon discussions with their representatives. This discussion points out the limitations of present vacuum systems with respect to satisfying stated objectives. This report also documents the effort which was directed toward evaluation of available ground-based vacuum facilities, and the subsequent conceptual design effort to develop advanced vacuum pumping systems when no suitable facility was identified. These advanced pumping methods would be suitable for use in a new ground-based MPD thruster test facility. As a part of the conceptual design effort, ANL contacted various vacuum system manufacturers' representatives to determine the current status and availability of vacuum pumping systems. This effort is discussed in a subsequent section, followed by ANL's evaluation of advanced pumping systems. Finally, rough cost and performance comparisons are made for the proposed candidate systems.

STATEMENT OF WORK

Argonne National Laboratory will do a research study and design a high altitude simulation test facility suitable for steady state MPD thruster operations and life tests.

- (1) The first phase will deal with advanced pumping concepts. Techniques shall be identified and evaluated for providing the very large pumping speeds required to test the MPD thrusters. System performance estimates shall be prepared to identify the most promising concepts.
- (2) The second phase will consist of a preliminary design study to determine the interactions between the thruster and the facility created by the operating MPD thruster. These effects may include, but are not limited to, induced magnetic fields, plume attachment to chamber walls, and induced voltages in the electrical lines. These interactions of the thruster with the chamber shall be used to establish design criteria to be used in Phase III.
- (3) The third phase will be the conceptual design of the facility. This shall consist of the design of the test chamber, pumps, support equipment, DC power supply, and data acquisition system to measure thruster primary performance characteristics, such as thrust, specific impulse, electrical to thrust power conversion, propellant flow rate, plume studies, erosion tests, and heat flux measurements. Criteria established in Phases I and II shall be employed in developing this conceptual design.
- (4) A cost effectiveness determination shall be made for the system. Each must be weighed by its merits as well as cost and impact upon the rest of the system. An ongoing facilities search shall also be made to locate existing facilities which could meet the test requirements as an alternative to new construction/procurement.

DELIVERY SCHEDULE

ANL shall prepare for AFRPL the following:

- (1) Three copies of a monthly technical letter on or before the fifteenth day of each month, covering the preceding month.
- (2) Three copies of a monthly financial status report on or before the fifteenth day of each month, covering the preceding month.
- (3) A technical presentation to AFRPL, at the conclusion of Phase I, to determine the feasibility of being able to design a test facility capable of meeting the test requirements.
- (4) A technical presentation to AFRPL, at the conclusion of Phase III, and one copy of a final report, no later than three months after the conclusion of effort. The final report should include a conceptual design of the test facility as well as a cost analysis and cost trade-offs. This final report will be used to compare the advantages/disadvantages of a ground test facility versus a space test platform.

SYSTEMS REVIEWED

CONVENTIONAL PUMPING SYSTEMS

A large number of pumping systems (and combinations of subsystems) were reviewed, based upon literature made available by, and discussions with, commercial vacuum system representatives. These systems are discussed in the following paragraphs with the intent of showing the logic which resulted in the elimination of most of them. (Note that the initial volume flow rate requirement was only 10^6 l/s at the initially required vacuum level of 10^{-2} torr compared to a flow rate of 4×10^7 l/s at a vacuum level of 10^{-4} torr.)

Roots Type Mechanical Pumps

Various manufacturers make large meshed-lobe (Roots) vacuum pumps in a wide range of volume rate capacities. These mechanical blowers are usually staged to accommodate the overall pressure ratio, with smaller sizes and a lesser number of blowers used in the higher pressure ranges. The largest Roots pumps have volume rate capacities in the range of 20,000 to 60,000 l/s, but are limited in pressure gain to a few torr from a lower range of 10^{-4} torr. Power requirements and casing overheating become excessive if pressure ratio is increased beyond design limits. Only the first stage of a mechanical vacuum pumping system need be considered in scoping calculations because subsequent stages of mechanical pumps become inconsequential in size and cost compared with the first stage due to the great reduction in volume flow rates at the higher pressures. For the initial system (10^{-2} torr) with a volume flow rate of 10^6 l/s, 20 to 60 of the largest mechanical pumps would have been required for the system. However, the practicality of providing ducting of sufficient flow area to the pump inlets was questioned even for this phase of the test program, since several "acres of pumps" were envisioned. The conductance losses of the vacuum piping would have been so severe that even more pumps (than noted above) would have been required, unless the piping were nearly as large in diameter as the vacuum vessel itself. When the required steady state vacuum level was changed to 10^{-4} torr, the number of mechanical pumps became even more impractical, so this type of pumping system was abandoned as unworthy of further consideration.

Oil Vapor Diffusion Pumps

Many manufacturers make diffusion pumps with sizes up to 1.22 m (48 inches) in diameter. Table 2 shows pumping capacities of typical oil vapor diffusion pumps (from Varian Corporation) with a range of 384 mm to 890 mm diameter. The unit-area capacity of these pumps at their choking limit is seen to be nearly constant (decreasing slightly with larger pumps). Since diffusion pumps are not effective at inlet pressures above 10^{-3} torr (see Figure 2), they were not considered for the initial vacuum condition. For the later requirement of 10^{-4} torr, a pump inlet area of nearly 60 m^2 would be

required for a volume flow rate of 4×10^7 l/s. When conductance and cold trap losses are considered, the inlet area increases beyond 100 m^2 . Thus, several hundred of the largest oil vapor diffusion pumps would be required to handle the gas load at the required pressure and at ambient temperature, with some margin from choking. These parameter values eliminate diffusion pumps from further consideration.

Turbomolecular Pumps

Pumping speeds of turbomolecular pumps range up to 9000 l/s for a 750-mm (30 inch) inlet diameter. These pumps have a flat pumping speed characteristic over a pressure range from 10^{-10} to 10^{-3} torr. A typical pumping characteristic curve obtained from the Balzers catalog is shown in Figure 3. This pumping curve shows that turbomolecular pumps "choke out" with back pressures of the order of 1 torr, and have to be protected from inlet gas pressure higher than 10^{-2} torr to preclude motor burnout. With a volume flow requirement of 4×10^7 l/s, a total of 4000 of the largest turbomolecular pumps would be required. This large number makes their use too costly and impractical.

Steam Ejectors

Though steam ejectors are widely used in industry for moderate vacuum service (approximately 1 torr minimum absolute pressure), they are capable of operation to considerably lower pressure levels. Figure 4 shows typical "pressure versus steam-to-gas mass flow ratios" for different commercial ejector designs from Croll-Reynolds Corporation. This figure shows that the ratio of steam required to exhaust air (or argon) at pressures down to 3×10^{-3} torr is of the order of 3000 to 1. For 6 g/s of argon, a flow of 18 kg/s of steam would be required. Though this flow rate is not impossible, it is considered excessive and would require a large dedicated steam supply. This conclusion is even more certain in view of the fact that the vacuum pressure requirement was extended to the 10^{-4} torr level and consequent steam requirements would increase by approximately a factor of ten. In the early work of this program, a combination of steam ejectors in the high vacuum portion of the system with liquid-ring roughing pumps seemed to be a possibility. Much of the steam requirement would have been eliminated by the liquid ring pump which acts both as a steam condenser and vane-type gas compressor. According to Kenney Vacuum Corporation (Ref. 10), the use of steam in ejector systems at moderately high vacuum is made practical by use of electrical heaters on the expansion nozzles to keep them from icing. Calculations were made for staged steam ejector systems with and without liquid ring pumps, using a standard ejector computer design program to determine performance characteristics. The performance capability depicted in Figure 4 was verified. However, further consideration of the use of steam ejectors was abandoned when the pressure level requirement was lowered and use of argon gas in a recirculation mode at low pressure was seen to be a rational alternative which offered additional advantages as will be discussed later.

Large Modified Axial Turbocompressors

Use of the compressor sections from surplus jet engines (J-57's) was briefly considered at the start of this program. At an equivalent inlet "Mach #" of 0.5, the pumping speed of one compressor would be over 60,000 l/s. Ten of these units driven at 9,000 RPM by modified starter motor drives (each developing ten horsepower at twice nominal rated rotation speed) would permit operation of the vacuum facility in the low 10^{-2} torr pressure range. Again, operation at even lower pressures precluded further consideration of this pumping scheme as first stage units.

Oil Vapor Booster Pumps

The vacuum industry developed a variant of diffusion type vacuum pumps approximately thirty years ago to handle large gas flows at moderate vacuum levels, called "oil vapor boosters." Constant pumping speeds up to 22,000 l/s over a range of inlet pressures from 10^{-2} torr to 10^{-4} torr can be obtained from existing designs of nominal 36 inch inlet diameter. A typical operating characteristic curve and equipment layout is shown in Figure 5 for an Edwards High Vacuum Company system (Model 100B4). The largest sizes of oil vapor booster pumps have not been built for the last ten years by either the Edwards company or by CVC, which has a comparable design. However, both companies stated their willingness to resume production given enough volume of business (perhaps ten or more units). By themselves, the maximum capacity oil vapor booster pumps do not have enough pumping speed to attain a 10^{-4} torr pressure level at argon flow rates of 6 g/s. Some 720 units would be required for this set of operating conditions. However, the oil vapor booster pumps lend themselves to become intermediate stages in a vacuum pumping system described later as one alternative to achieve the requisite vacuum and flow capability.

Cryogenic Vacuum Pumps

Commercial vendors supply vacuum pumping systems based upon cryopumping -- gases and vapors condense on cold surfaces in a batch mode of operation. Units are available from several manufacturers with pumping speeds in the range of 20,000 to 30,000 l/s. Special designs could probably be obtained for even larger unit pumping speeds. However, the high flow rates of condensibles in the proposed system would limit the net operating time of the vacuum system to approximately an hour between regenerations. This unacceptable operating characteristic of commercial cryopumped systems led to the "continuous cryopumping" concept which is proposed as an alternative later in this report.

VACUUM SYSTEM CONSIDERATIONS

The plume which emanates from an MPD thruster may have a wide range of expansion characteristics, depending upon choice of thruster design and MPD

operating parameters. In attempting to provide a physical vacuum system which can accommodate a reasonable sampling of thruster designs, a number of assumptions about plume characteristics had to be made. Also, some of the plume characteristics could be inferred from other known parameters. The vacuum chamber reference design (i.e., size of tank) was made with the assumption of a fully expanded plume. Using literature values (Ref. 11) of specific impulse, jet velocities are obtained. Using data which indicate that approximately 90% of the momentum is due to magnetoplasma interaction effects, the "thermal expansion" energy is inferred. This energy allows calculation of an equivalent thermodynamic temperature. Knowing the equivalent plume thermodynamic temperature and system static pressure, equivalent gas density is calculated. Plume area is then calculated from the gas mass flow, density, and velocity according to the mass continuity equation. It appears that plume expansion to a diameter of 3 to 4 meters is likely for this extreme case. The vacuum tank diameter must be larger than the plume to accommodate it and auxiliary equipment. For a reference tank design using rolled aluminum sheet, a tank diameter of approximately 5.8 m can be obtained with a single longitudinal weld. Arbitrary tank length is obtained by stacking ring sections and using girth welds. The question of arc interaction with a metal (conducting) tank was not addressed in the present study. Either a nonmetallic (insulator) lining could be used to preclude arcing to the walls, or the tank could be made from some nonconductor with appropriate strengthening. A preliminary stress analysis showed that an aluminum tank (5.8 meter diameter and 20 meter length) having 25 mm wall thickness and five ring-type stiffeners on 3 meter axial spacing could withstand vacuum induced forces while providing sufficient porting space for vacuum pump connections. Since the MPD thruster facility requires a power supply, a cooling water supply, and other support facilities in addition to a building to house them, the vacuum system sizing was done keeping an available experimental area at ANL in mind. An enclosed high bay building having a floor area of 30 m by 40 m with a free height (below a 10-ton bridge crane) of 10 m is compatible with the above design parameters.

torr. Achieving a plume static pressure level less than 10^{-4} torr using only preboosters and oil vapor boosters was found to be impractical.

It was concluded that a means had to be found to boost the inlet pressure to the pumping system. Pressure recovery using a diffuser appeared to be practical. The assumption has been made that some pressure recovery (a multiplying factor of three to five) would be obtained in a supersonic diffuser located between the thruster's exhaust plume and the inlet to the first-stage pumps. Such a diffuser is a required item for each of the proposed vacuum systems, and the common design requirements are discussed later. Suffice to say that the pressure ratio of the diffuser required for the argon prebooster system is modest in terms of potential pressure recovery. The general "rule of thumb" in hypersonic low Reynolds number flow (in the continuum flow regime down to transition flow) is that 80% of a normal shock pressure ratio is possible. At Mach No. equal to 7, a pressure regain of fifty is thus possible, based upon a reference to upstream static pressure. We hope to attain roughly one-tenth of this pressure ratio at the lower operating pressure levels of interest. The volume flow rate (shown in Table 4) at the inlet to each stage of pumping is seen to constantly decrease, even though more argon gas is being recirculated at each stage to drive these ejectors. After Stage 3, the volume flow has been reduced to approximately half of the inlet capacity of one of the large oil vapor boosters. This reduction in volume flow rate is accomplished both by an increase in pressure, and by a decrease in the absolute temperature due to mixing warm vacuum tank effluent with cold driver expansion gas. Despite mass flow increases in the prebooster system, mixing cold expansion flow from the driver nozzles has a significant effect in reducing the mixed gas temperature and absorbing enthalpy. The prebooster stages will be insulated from the warm ambient to take full advantage of this effect. Figure 6 displays the information in Table 4 in block format and adds information about interstage pressure, temperature, flows, and calculated sizes of passages. Flow lines in Figure 6 also show that the recirculated argon gas goes to each ejector driver through electric heaters that are needed to preheat the argon to optimize the jet expansion process; using ideal gas law thermodynamic relationships, near optimum temperature, pressure, flow area, and velocity values are derived and recirculation argon flow is minimized.

The referenced vacuum tank and pumping system, constructed from commercially available equipment, are shown in Figure 7 (side view, end view, and partial cutaway top view of the tank and oil vapor booster pumps). As configured, this system can achieve pressure levels in the low 10^{-2} torr range with 6 g/s of argon flow. Ten parallel pumping systems are pictured. Provision for two additional pumping systems (total of twelve) is depicted in the side porting. The oil vapor booster pump systems are connected into a common discharge manifold which serves a number of functions: (1) fewer (four) mechanical backing pump systems (one redundant) are required; (2) any oil vapor discharged with the booster exhaust will condense and drain back into the booster boilers for recovery; and (3) the recirculated argon flow can be

PROPOSED ADVANCED PUMPING SYSTEMS

Three different vacuum pumping system concepts were developed during the course of the present study. These include (1) an argon gas prebooster system coupled with oil vapor booster pumps and mechanical backing pumps, (2) a continuous cryogenic vacuum pumping system, and (3) an axial linear magnetic induction plasma pump. These concepts are described in following sections. Table 3 presents a summary of the key features of the three concepts.

ARGON PREBOOSTER/OIL VAPOR BOOSTER COMBINATION

The oil vapor booster designs available from several commercial companies cannot by themselves meet the simultaneous requirements of pressure and flow for the MPD thruster (approximately 720 units would be required). Use of a set of staged ejectors ahead of each of the oil vapor boosters was considered in order to reduce the required number of units and achieve the required pressure and flow conditions. Argon was chosen as the working gas in these ejectors because it would already be available within the vacuum system at the required subastrospheric pressure, and because argon has desirable vapor pressure and expansion characteristics. Argon would not condense or freeze out in expansion through large pressure ratios in the driver nozzles of the ejector systems. Calculations were made (included in the Appendix) to show the optimum flows, driver stagnation pressure levels, and sizes of the staged ejectors used ahead of the oil vapor boosters. A standard ejector program (Ref. 12) was used to size each of the ejectors based upon the knowledge that the driver flows are within the continuum flow regime through their respective nozzle throats. The expanded supersonic flows are mainly within the transition flow region. Corrections for wall effects will have to be made in designing ejector driver supersonic nozzle bells; this was not done at the present level of effort. The shapes of the ejector suction sections were derived from the shapes of commercial ejector systems for the low pressure stages. A summary of the prebooster stage conditions are tabulated in Table 4. A block diagram of system operating conditions including the three argon prebooster stages, the oil vapor boosters, and the two mechanical stages of vacuum pumps is shown in Figure 6 (typical of each of the 10 or 12 parallel flow pumping systems). A layout of the oil vapor booster and referenced vacuum system is shown in Figure 7. The modifications which are required to add the argon preboosters to the oil vapor booster system are shown in Figure 8.

A number of prebooster system characteristics of interest are given in Table 4. The driver pressures of the argon ejectors range from a fraction of one torr to approximately ten torr. This means that the recirculated argon gas can be supplied, for example, from the exhaust system at an intermediate pressure below atmospheric. The outlet pressure of 50 torr from the Roots blower stage seems to be ideal; adequate pressure margin is available for flow losses and control of flow rate in the driver supplies to individual ejectors. The inlet pressure to the first stage of argon prebooster is higher than 10^{-4}

ballasted around the first-stage mechanical pumps from this reservoir to provide a stable intermediate pressure argon source. The vacuum tank itself has dished heads which are removable. Standard compression-type elastomer seals are used with bolted lugs to fasten the heads and shell. The shell is considered to be nominal 25 mm (1 inch) aluminum plate in this referenced design which is fabricated from single sheets with a single longitudinal weld, and with girth welds between the formed ring sections under each of the reinforcing rings. A preliminary stress analysis was performed. Arc interactions have not been addressed in this study except for the recognition that an insulating liner would be provided. The electrical power requirement for the pumping system could range upwards from 1 megawatt (each oil vapor booster requires 90 kW maximum).

Operating pressure level versus mass flow rate is shown in Figure 8 for a progressive series of vacuum system designs. Flow capacity curves are shown in Figure 8 for two and ten oil vapor boosters, and for ten argon prebooster/oil vapor booster vacuum pump sets. These pumping systems can be compared with the Stuttgart facility and with the desired MPD thruster operating point. A diffuser having a pressure recovery factor of three (or more) is considered necessary to meet the desired operating condition.

The addition of argon preboosters to the basic vacuum tank and oil vapor booster system is shown in Figure 9 in partial detail. In this conceptual design, the oil vapor booster pumps are moved outward from the tank, turned 180 degrees, and the three stages of prebooster ejectors interposed. The vacuum tank is raised in elevation to allow centerline porting. In order to "package" the preboosters in an available building, the first stage had to be designed for minimum volume and length. Thus, the first stage of the prebooster system is a disk-shaped ejector with a ring-type driver manifold-nozzle as shown in detail C-C of Figure 9. The performance of this annular flow first stage is expected to be less than that of a coaxial ejector (Ref. 13). The second and third stage ejectors are coaxial with the discharge ducting, with separation distances and angles sized with reference to commercially designed diffusers for multistage oil vapor diffusion pumps. The argon prebooster/oil vapor booster combination pumping system (with diffuser) offered a clean (from a contamination standpoint), most controllable, most energy efficient, and most compact packaged vacuum system that promised to meet the stated vacuum and flow rate requirements.

CONTINUOUS CRYOPUMPING SYSTEM

A number of cryogenic fluid cooled "cryopumping" systems were considered. Commercially available pumps are limited in capacity ($\approx 20,000$ l/s) and must be periodically regenerated, necessitating shutdown at regular intervals.

Cryopumping is based upon the fact that gas molecules will stick to surfaces that are significantly below the gas triple point temperature. The saturation vapor pressure of argon is less than 10^{-6} torr at 30 K. Gas flow

to the cryopanel is essentially sonic so that the flow rate capacity of the cryopanel is dictated by the static pressure (vacuum level) and the available projected area (normal to the flow). Bailey (Ref. 14) derives cryopumping capacity relationships; his criteria were used to size the following cryogenic systems.

Figure 10 depicts an early concept of an ANL-designed cryopumping system which also suffers from the "batch mode" requirement for regeneration. In this concept, the MPD thruster plume flows through a supersonic diffuser/enthalpy extractor which recovers pressure and removes most of the enthalpy of the plasma. (The diffuser is described later in this report.) The cryopanel is depicted as a double surface panel operated at 30 K, sandwiched between two chevron panels at 77 K. The 30 K cryopanel is cooled by gaseous helium from a recirculating system that includes an external commercial compressor, heat exchanger, and engine-expander refrigeration system. The two chevron radiation heat shields are cooled by liquid nitrogen supplied from an external dewar system. Plume flow-out of the diffuser is at subsonic velocity and either impinges directly on the front face of the cryopanel or flows around to the back face and condenses there. The enthalpy load from the condensing and solidifying gas (argon flow rate of 6 g/s) is less than 1000 watts, of which 15 watts are due to radiation and conduction heat losses from the surroundings. Approximately 70% of the cryopanel "speed" is obtained at the front surface. At this flow rate of 6 g/s, the solid argon buildup exceeds one millimeter per hour. With solid argon buildup, pumping effectiveness diminishes, limiting test time. Therefore, a continuous cryopumping system was considered to be necessary.

Figure 11 depicts a modification to the referenced vacuum system of Figure 10 which incorporates a mechanical scraper and solid argon removal system. One or more radial arms having sharp "doctor blades" physically scrape the accumulated solid argon from the surface of the cryopanel at time intervals that are short compared to a critical buildup time (one hour). Thus, the cryopanel surface is continually "renewed" in its effectiveness. From thermodynamic/kinetic considerations, the argon is expected to be frozen out in the form of "snow" rather than a tenacious "hard ice" film (Ref. 15). The scrapings of solid argon fall into a cryocooled receptacle located above a cryogenic valve. By opening and closing the cryocooled valve, the solid argon is deposited periodically into the bottom chamber which is alternately cooled and warmed. During the warming process, the argon is vaporized and pumped out through the exhaust system.

In Figure 12, a second continuous cryopumping concept is presented. This concept features a "thermal scraper" for the solid argon. A single radial "omega" shaped duct (see Figure 13 for cross-sectional detail) moves azimuthally around the cryopanel surface. An electric heater in the duct supplies thermal energy at a rate which is proportional to radius, and at rates (<1 kW) that are sufficient to vaporize the resident solid argon stored within a honeycomb

structure bonded to the cryopanel face. Lip seals on each side of the omega channel limit leakage flow back into the vacuum chamber to insignificant amounts. A coaxial duct connected to the radial omega duct is used with a rotating seal to pipe the gasified argon directly to roughing pumps. This cryopumping system feature results in an argon pressure rise from the low 10^{-4} torr range up to 10 torr for external pumping by a small capacity roughing pump (60 l/s).

AXISYMMETRIC LINEAR INDUCTION PLASMA PUMP (ALIPP)

The plasma pump concept is based upon using an electromagnetic (EM) pump to raise the pressure of the plasma in the vacuum chamber. (EM pumps are commonplace in liquid metal pumping systems.) In the present case, the pumped fluid is the ionized plasma from the MPD thruster. (At high temperatures, the gas is fully ionized and becomes a plasma.)

The function of the EM pump is to lower the velocity while raising the pressure of the MPD plume from approximately Mach number = 6 and pressure equal 10^{-4} torr to a subsonic velocity and a pressure that matches the downstream pumping system. However, high Mach number and low pressure conditions are maintained at the thruster end of the chamber while the subsonic high pressure condition (10^{-1} to 1 torr) prevails at the downstream end, where a conventional mechanical pumping system can handle the gas load.

The physical layout of the ALIPP is shown in Figure 14. The reference vacuum tank is fitted with a series of solenoid wound field coils along the axis around the inner periphery of the vacuum tank. It is expected that, due to the radial forces generated by ALIPP, the plasma will be confined near the core of the tank without touching the coils. An "egg crate" type diffuser/heat exchanger (enthalpy extractor), described later, is located downstream of the field coils and ahead of the external vacuum pumping system. Reference 16 proposes a similar device for plasma acceleration and briefly discusses the principle of operation where a traveling wave is applied to the plasma. In Ref. 17, a one-dimensional analytical model was developed for performance predictions of a traveling wave EM pump and some results were presented. In Ref. 18, experimental results were presented showing that a similar device, operating as a plasma accelerator, could be operated at roughly 50% efficiency. In the traveling wave pump, electrodes do not contact the plasma, which is a major advantage because electrodes are usually subject to rapid erosion at the current densities considered for plasma propulsion.

In general, such a device can be operated either as an accelerator or as a pump, depending upon the particular application and the boundary conditions downstream of the flow. In the accelerator mode, it accelerates the flow to supersonic velocities, whereas in the pump mode flow is decelerated to possibly subsonic velocities, depending on the downstream pressure. According to Ref. 19, in the pump mode, enthalpy, pressure, and gas density all rise along the direction of flow while velocity falls.

Reference 20 gives a rather detailed analytical treatment of annular linear induction pump for liquid metal applications. Referring to Figure 15, the operating principle of the ALIPP can be understood as follows. A series of coils are placed inside the vacuum chamber far enough downstream of the thruster so as not to disturb the exhaust plume. A three-phase alternating electric current excites the coils and generates a traveling magnetic field which propagates along the part of the chamber which contains the coils. The shape of the B-field lines at one instant in time is shown in Figure 15. Both radial and axial components of the magnetic field exist at most points inside the coils. Because of the axial symmetry, there is no azimuthal magnetic field. Through Maxwell's equations in the following form,

$$\frac{\partial \vec{B}}{\partial t} = - \vec{\nabla} \times \vec{E}$$

the time varying B-field induces azimuthal current flow in the ionized plume of the MPD thruster. This current interacts with the axial component in the B-field to produce radial forces on the plume. The induced current also interacts with the radial component of the traveling field to produce the desired axial pumping force on the plume.

The axial pumping force per unit volume is proportional to the plasma conductivity (σ), the strength of the radial component of the B-field (B_r), and the difference between the plasma velocity (V_p) and the wave velocity (V_w) of the traveling field as follows:

$$F \sim \sigma(V_w - V_p)B_r^2 .$$

If the traveling magnetic wave is moving faster than the plasma, the pumping force will be in the direction of motion of the plasma. If the downstream pressure is low, the plasma will accelerate and can reach supersonic velocities; in this case the device acts as an accelerator. On the other hand, if the downstream pressure is higher than upstream, the device will act as an EM pump, thereby slowing the gas while increasing pressure, which is the objective.

A rough estimate of the performance of this device shows that, for a radial component of the magnetic field (B_r) of 1000 gauss (0.1 Tesla), a plasma conductivity of 10 S/m (corresponding to an argon temperature of 3800 K and pressure of 10^{-4} torr, per Figure 16), and a relative velocity of 25,000 m/s, a pressure gradient of 2500 N/m^3 (18.8 torr/m) is possible. So it seems quite possible to maintain an overall pressure distribution in the vacuum chamber having 10^{-4} torr at the MPD thruster exhaust and 10^{-1} to 1 torr at the outlet of the ALIPP.

However, for the ALIPP to work as intended, the applied traveling B-field must penetrate the plume to apply the Lorentz ($\vec{J} \times \vec{B}$) body force on the ionized gas. This can occur if the magnetic Reynolds number is small or moderate. In

this case, the applied traveling magnetic field will penetrate the plasma to a distance referred to as the skin depth (δ). The skin depth is inversely proportional to the product of the plasma electrical conductivity (σ), the plasma permeability (μ), and frequency of the traveling wave (ν). The skin depth (δ) is given by the following relation:

$$\delta = (2/\sigma\omega\mu)^{\frac{1}{2}}$$

where $\omega = 2\pi\nu$.

Figure 17 presents the variation of the skin depth as a function of argon temperature (conductivity) with the AC frequency of the traveling field as a parameter. There is flexibility in selecting feasible frequencies and skin depths.

According to the behavior described above, the overall flow field will appear as follows. The plume entering the ALIPP will be at a Mach number = 6 and at a static pressure of 10^{-4} torr. The plume will be decelerated by the ALIPP to approximately Mach number = 1 (or lower). In this region of the ALIPP operating characteristics, the electromagnetic forces on the plume will be pushing the plume forward while increasing gas density and pressure. In other words, the ALIPP will act on the plume in a classical pumping fashion; it will add energy to the flow by further increasing the pressure and density while reducing the velocity accordingly. The traveling wave speed is set by the requirement that the ALIPP exhaust velocity be sonic at the discharge pressure, as set by the vacuum pump backing system (0.1 to 1 torr). The remaining ALIPP parameters, such as the traveling field wave length, the field strength, and the overall coil structure length, are set by optimally matching the ALIPP discharge pressure with the backing system pressure.

It is anticipated that adequate electrical conductivity will remain in the MPD thruster plume to satisfy feasibility requirements. If further work shows this to be questionable, a reduced conductivity can be compensated for by either increasing the magnitude of the traveling wave B-field or by reionizing the plume. A number of means can be employed to reionize the plume, such as microwave heating, electron-cyclotron or ion-cyclotron resonance heating, electrothermal heating by a separate E- or B-field system (Ref. 21), or perhaps by reionization of the gas along the first few coils of the ALIPP itself (Ref. 18).

A final point should be mentioned. The previous discussion has been developed under the assumption that the plasma being pumped by the ALIPP is a relatively dense, collision dominated, continuum gas. This is most probably true in the core of the plume but, near its edges and outside the plume, the gas entering the ALIPP will be at an equilibrium pressure of roughly 10^{-4} torr. In this annular region around the MPD plume, free molecular flow prevails and the mean free path is approximately 50 cm (Ref. 22). However, ions and electrons will be pumped by the traveling B-field as they spiral around

the field lines at their respective Larmor radii. Further investigation of this point is needed.

GASDYNAMIC DIFFUSER/ENTHALPY EXTRACTOR

All of the proposed candidate pumping concepts need a gasdynamic diffuser/enthalpy extractor to operate within the MPD thruster requirements of 6 g/s flow of argon at an ambient static plume pressure of 10^{-4} torr. The argon prebooster and oil vapor booster combined system and each of the cryo-pumping systems need a gasdynamic diffuser that is located upstream of the active pumping system. The ALIPP pump needs an enthalpy extraction heat exchanger downstream of the solenoid coil structure; gas diffusion with the intent of additional pressure recovery is a lesser requirement with the ALIPP system than with the others.

Design of the diffuser structure is entirely dependent upon the plume size and enthalpy load. If the plume is fully expanded within the vacuum chamber, the plume's dynamic head is at a minimum; also, local heat transfer loads in terms of heat fluxes to the diffuser are lowered. The diffuser concept for this study is shown in Figure 18. It was designed for the largest plume expansion case in order to size the vacuum vessel. The integrals of enthalpy extraction and pressure recovery throughout the diffuser and the coupling between them as a function of plume size are unknown. However, some trends can be predicted a priori to testing prototypic hardware. With a condensed (small diameter) plume, the dynamic head will be increased due to the high density of the gas even if velocities remain invariant. It would be expected that a higher absolute pressure recovery is possible with a plume that is concentrated near the axis of the diffuser structure. With the concentrated plume, the heat transfer from ionization energy deposition on diffuser structure would be higher -- again corresponding to the higher plasma density. There is an indication (Ref. 23) that the plume expansion characteristic is dependent upon controllable thruster design parameters and upon controllable magnetic interaction parameters; also the heat fluxes from a dense plume could be expected to be extremely high and concentrated near the leading edge of the structure. Thus, a first design of the diffuser might opt for a plume that is concentrated as much as possible to achieve the highest degree of pressure recovery but keeping heat fluxes within established cooling capabilities. Existing convective cooling methods can handle approximately 20 kW/cm² routinely. (Higher fluxes can be tolerated under special circumstances.) With an enthalpy load within the plume of approximately 2 or 3 megawatts (from 6 g/s of argon plasma considering an approximate 50% energy transfer from the arc to the gas), the enthalpy should be spread out over an area of at least 150 cm². A minimum plume diameter is probably 30 cm according to this criterion (and the supposition that deionization heat fluxes correspond linearly with potential flow characteristics). It is further assumed that the major portion of the total enthalpy extraction (ionization energy) will take place near the leading edge of the diffuser. The remaining

thermal energy will be dissipated along the remaining surface of the diffuser according to classical heat transfer correlations. With these assumptions, the pressure recovery is seen to be essentially decoupled in effects from the enthalpy extraction, unless "bow shocks" are set up by the "deionization flows" at the diffuser inlet. To determine whether this will occur is the legitimate objective of future experiments.

(Remarks: Hypersonic low Reynolds number flow within a constant area diffuser has not been studied extensively within the free molecular and transition regimes that would characterize operation of the proposed facility. The mean free path of the gas molecules is of the order of the lateral dimension of the diffuser elements. The extent of "analysis" conducted in Phase A was consultation with rarified flow gas dynamicists who had experience in continuum hypersonic flow at low Reynolds number. "Rules of thumb" were extrapolated generously with a corresponding severe "safety factor" applied to estimated pressure ratios.

We do not anticipate a defined "shock structure" in the straight duct diffuser elements -- the starting mean free path (MFP) is too long. At a shock thickness of 5 to 10 MFP, the shock would be nearly as thick as the design length of the diffuser (20 diameter). Wall interaction effects that define pressure loss/gain will probably require analysis based upon Monte Carlo techniques, since integral equations are involved. This extent of analysis was beyond Phase A funding limits.)

COSTS

Certain building, services, and systems features are common to the three concepts described previously. The costs for these encompass the following items:

- Building
- Installed electrical power and services
- Vacuum chamber
- Gasdynamic diffuser
- Mechanical roughing/backing system
- MPD thruster power supply

Three vacuum pumping concepts have been described, all sharing the common features described above. They are

- Argon Prebooster/Oil Vapor Booster Pumping System
- Continuous Cryogenic Pumping System
 - Mechanical scraper
 - Thermal scraper
- Axisymmetric Linear Induction Plasma Pump (ALIPP)

Costs are presented for preparation of the building and necessary services. Costs for complete MPD thruster test facilities located in the building are presented separately for purposes of comparison. The cost estimates are based upon the referenced designs, which assume that development and testing of critical components have been completed. All costs are rough estimates, based upon minimal conceptual design, and should be used for early planning purposes only. Contingency and escalation are not included. Facility operating cost and consumables are not addressed here; they will be treated when there is better definition of the facility.

COMMON COSTS

Facility Costs

Building and Services Costs:

- | | |
|--------------------------------------------------------------|------------|
| • Auto-transformer and cables for MPD thruster power supply: | \$200K |
| • Cooling water, etc., connections: | 20K |
| • Building preparations: | 20K |
| • Miscellaneous small items: | <u>10K</u> |

Total cost for housing the Test Facility: \$250K

Components Common to All Systems

Major Procurements:

- Vacuum chamber with insulated lining
(chamber dimensions: 20' dia x 60' long): \$380K
- Diffuser (10' long x 19' dia): 312K
- Representative mechanical roughing/backing
system comprising 4 modules, each of which
contains a Roots blower, mechanical pump,
interconnecting piping, and electropneu-
matic valves (cost/module = \$50K): 200K

Total cost of procured common items: \$892K

Installation:

Miscellaneous material \$ 20K

Engineering:

- Staff and technical support for design
and procurement of common major items: \$300K
- Staff and technical support for installa-
tion of common major systems: \$150K

Total Installation & Engineering Costs \$470K

Total Common Components Costs (installed cost
of vacuum chamber, diffuser, and roughing/
backing system): \$1362K

ARGON PREBOOSTER/OIL VAPOR BOOSTER SYSTEM

Major Procurements:

- Ten oil vapor booster pumps
(cost/pump = \$150K) \$1500K
- Ten 36-in. elbows (cost/elbow = \$10K) 100K
- Ten elongated reducers
(cost/reducer = \$20K) 200K
- Ten bellows (cost/bellows = \$10K) 100K

Total cost of procured items: \$1900K

Fabricated Parts:

- Ten sets of prebooster details
(\$37.2K/set) \$372K
- Miscellaneous details 37K

Engineering:

Staff and technical support for design,
fabrication, and installation: \$211K

Total costs for Fabricated Parts & Engineering \$620K

Installed Cost of System (procurements
plus fabrication plus engineering) \$2520K

Common Costs (from A.2 above) + 1362K

Subtotal \$3882K

Assume I&C cost is 15% of Subtotal + 582K

Total installed cost of **Argon Prebooster/Oil Vapor
Booster System** excluding building and services costs: \$4464K

CONTINUOUS CRYOGENIC SYSTEM

There are two continuous cryogenic pumping system concepts, namely, the mechanical and the thermal scraper designs. They are similar in scope and share many common features so that cost differences are small. Accordingly, only the mechanical scraper costs are presented.

Major Procurements:

- Helium Refrigeration System delivering
20K gaseous helium with a capacity of
1000 watts of cooling at the cryopanel: \$450K
- Cryogenic piping and plumbing: 100K
- Cryogenic gate valve: 16K
- Motor drive and seals, etc. 20K

Note: The liquid nitrogen supply for the
radiation shields will be a leased
system and included as part of the
operating costs.

Total cost of procured items: \$586K

Fabricated Parts:

- Cryopanel (19' dia): \$60K
- Radiation shields and baffles: 68K
- Special dewars: 27K
- Scraper: 12K
- Miscellaneous parts: 20K

Engineering:

Staff and technical support for design, fabrication, and installation:	\$300K
Total costs for Fabricated Parts and Engineering	\$487K
Installed Cost of Cryogenic System (procurements plus fabrication plus engineering)	\$1073K
Common Costs (from A.2 above)	+ 1362K
Subtotal	\$2435K
Assume I&C cost is 20% of Subtotal	+ 487K
Total installed cost of Cryogenic Pumping System excluding building and services costs:	<u>\$2922K</u>

ALIPP SYSTEM

Major Procurements:

Power supply (100 kW, 100 kHz):	\$600K
---------------------------------	--------

Fabricated Parts:

• Induction coil (19' dia, 20 turns/phase, 3 phase):	\$144K
• Cooling system:	50K
• Miscellaneous parts and cable:	50K

Engineering:

Staff and technical support for design and installation:	<u>\$250K</u>
Installed cost of ALIPP System (procurements plus fabrication plus engineering)	\$1094K
Common Costs (from A.2 above)	+ 1362K
Subtotal	\$2456K
Assume I&C cost is 20% of Subtotal	<u>491K</u>
Total installed cost of ALIPP System excluding building and services costs:	<u>\$2947K</u>

SUMMARY OF COST ANALYSES

The cost in FY 86 dollars to furnish each of the three systems is summarized in Table 5. Development and building preparation costs are included.

RATIONALE FOR PHASE II TEST PROGRAM

The Phase I effort resulted in conceptual development of three advanced vacuum pumping concepts for application to ground testing of MPD thrusters having flow rates up to 6 g/s, at a vacuum level of 10^{-4} torr, and with power dissipation by the thruster plume of several megawatts. Each of these advanced pumping concepts requires a diffuser/enthalpy extractor to operate at the stated vacuum and flow conditions. Consequently, priority development should be in this area. With a consistent specification of hardware and auxiliary equipment, testing would be performed on a subscale but still significant power, flow, and thrust levels to facilitate the amount of relevant design data to be obtained.

The test program to be undertaken in FY 1986 is constrained by a relatively low funding level. Existing AFRPL vacuum facilities, augmented by a megawatt power supply from ANL, are planned to be used to maximize the generation of useful data within that constraint. Since no thruster development can be undertaken, existing thruster(s) from Princeton will likely be needed. A basic consideration is that the test program should be planned so that the data applies to more than one pumping concept (preferably to serve as a discriminator between concepts) and helps in defining the parameters that go into the advanced pumping system design.

The discussions in the last section establish clearly the essential technical issues that need experimental resolution at the earliest stage of the program. Virtually all of the problems and concerns with the proposed concepts have to do with the interaction of the plume with the first solid surface encountered. This is independent of the pumping concept proposed. Very little experimental or theoretical information is available on the subject and it clearly forms the prime topic for early experimental study. A carefully constructed test program to address this issue can have significant implications not only on MPD thruster research but on other related R&D as well.

SUMMARY AND CONCLUSIONS

A conceptual design effort for specifying a ground-based moderate vacuum system having high flow throughput capability was conducted in support of the development of magnetoplasmadynamic (MPD) thrusters for space propulsion missions. Vacuum system manufacturers were contacted to assess the present status and availability of many types of commercial vacuum pump systems. Literature was surveyed to assess capability and availability of existing vacuum facilities. It was established that existing pumping systems and facilities are not able to meet the simultaneous requirements of MPD testing. Three advanced vacuum pumping concepts were developed which do meet the projected requirements of MPD thruster testing. All three concepts -- argon prebooster, cryopumping, and axisymmetric linear induction plasma pump (ALIPP) -- require the use of a gasdynamic diffuser/enthalpy extractor. This latter device must be developed as a preliminary to formal design of a new high flow capacity vacuum facility.

A review of the concepts developed was performed at Princeton University by Princeton and ANL personnel. A letter summarizing the results of the review (Ref. 24) has been sent to AFRPL. Briefly, the conclusion of the review was that the proposed concepts presented reasonable approaches to meet the demanding requirements for a steady state MPD thruster test facility. The primary unresolved issue was the nature of the interaction between the plume and the first physical surface it sees. This first surface interaction problem is now recognized as being universal to the design of all test facilities and represents a topic for which little theoretical or experimental information exists. A test program is being designed to address this question. Data from the proposed tests will be needed before engineering design of pumping concepts can be developed further.

REFERENCES

1. Kelly, A.J., Nerheim, N.M., and Gardner, J.A., "Electron Density and Temperature Measurements in the Exhaust of an MPD Source." AIAA Journal, Vol. 4, No. 2, pp. 291-295, 1966.
2. Bruckner, A.P., and Jahn, R.G., "Exhaust Plume Structure in a Quasi-Steady MPD Accelerator." AIAA Journal, Vol. 12, No. 9, pp. 1198-1203, 1974.
3. Maisenholder, F., and Mayerhofer, W., "Jet-Diagnostics of a Self-Field Accelerator with Langmuir Probes." AIAA Journal, Vol. 12, No. 9, pp. 1203-1209, 1974.
4. Michels, C.J., Rose, J.R., and Sigman, D.R., "Electron Number Density and Temperature in MPD-Arc Thruster Exhausts." AIAA Journal, Vol. 10, No. 11, pp. 1395-1396, 1972.
5. Michels, C.J., and York, T.M., "Exhaust Flow and Propulsion Characteristics of a Pulsed MPD-Arc Thruster." AIAA Journal, Vol. 11, No. 5, pp. 579-580, 1973.
6. Kimblin, C.W., "Cathode Spot Erosion and Ionization Phenomena in the Transition from Vacuum to Atmospheric Pressure Arcs." J. App. Phys., Vol. 45, No. 12, pp. 5235-5244, 1974.
7. Gabriel, S.B., and King, D.Q., "Thrust for Interorbital Propulsion: A Question of Lifetime," pp. 287-302 in Orbit-raising and Maneuvering Propulsion: Research Status and Needs, (Volume 89 - Progress in Astronautics and Aeronautics), Am. Inst. of Aeronautics and Astronautics, Inc, New York, 1984.
8. Williams, F.U., "Vacuum Chamber Survey," Appendix D to MPD Thruster Application Study, Eagle Engineering, January 1981.
9. Cassady, R.J., Private communication regarding "Technical Installations and Facilities of the Institute for Space Propulsion, University of Stuttgart," Air Force Rocket Propulsion Laboratory, Edwards Air Force Base, CA, 1984.
10. Dobrolowski, C. (Chief Engineer, Kenney Vacuum Corporation), Personal communication.
11. Vondra, R.J., Nock, K.T., and Jones, R.M., "A Review of Electric Propulsion Systems and Mission Applications." Paper No. IEPC 84-82 presented at the JSASS/AIAA/DGLR 17th Int'l Electric Propulsion Conference, Tokyo, 1984.
12. DeFrate, L.A., and Hoerl, A.E., "Optimum Design of Ejectors Using Digital Computers." Chem. Engr. Prog. Symp. Series, Vol. 55, No. 21, pp. 43-51, 1959.

13. Adkins, R.C., "A Simple Method for Designing Optimum Annular Diffusers." ASME Paper 83-GT-42, 1983.
14. Bailey, C.A., Advanced Cryogenics, Plenum Press, London, 1971.
15. Huffman, P.J., and Dietenberger, M.A., "Prediction of Ice/Frost Growth on Insulated Cryogenic Tanks." J. Spacecraft & Rockets, Vol. 20, No. 4, pp. 401-403, 1983.
16. Covert, E.E., and Haldeman, C.W., "The Traveling Wave Pump." ARS Journal, No. 31, pp. 1252-1260, 1961.
17. Covert, E.E., Boedeker, L.R., and Haldeman, C.W., "Recent Results of Studies of the Traveling Wave Pump." AIAA Journal, No. 2, pp. 1040-1046, 1964.
18. Heflinger, L., Ridgway, S., and Schoffer, A., "Transverse Traveling Wave Plasma Engine." AIAA Journal, No. 3, pp. 1028-1033, 1965.
19. Shercliff, J.A., A Textbook of Magnetohydrodynamics, pp. 194-198, Pergamon Press, Oxford, 1965.
20. Schwirion, R.E., An Analysis of Linear-Induction or Traveling Wave Electromagnetic Pumps of Annular Design, NASA TN D-2316, May 1965.
21. Jahn, R.G., The Physics of Electric Propulsion, McGraw Hill, New York, 1968.
22. Diels, K., and Jaekel, R., Leybold Vacuum Handbook, Pergamon Press, New York, 1966.
23. Jahn, R.G., Personal communication.
24. Bhattacharyya, S.K., Lazar, James, and Reed, C.B., ANL letter #ENG.AP-9396 to Lt. Orin Kilgore (AFRPL) concerning "Argonne National Laboratory: Princeton University Review of Advanced Pumping Concepts for Use in MPD Thruster Test Facilities," December 4, 1985.

Table 1. Large Vacuum Facility Characteristics

Location	Size		Pumping	Cooling	Pressure Level
	Diameter	Height			
Langley, Virginia	55'	55'	Diffusion Pumps	None	10^{-4} torr
Lewis Res. Ctr., Space Prop.	42'	70'	Diffusion Pumps	None	10^{-7} torr
Lewis Res. Ctr., Space Power	100'	122'	Diffusion Pumps	400 kW	10^{-6} torr
NASA, Houston	65'	120'	Diffusion and Cryogenic Pumps	7 kW	10^{-7} torr

Table 2. Diffusion Pumps

<u>Model No.</u>	<u>ID (mm)</u>	<u>Area (m²)</u>	<u>Capacity (torr-liter/s)</u>	<u>Capacity Area (torr-liter/m² s)</u>
VHS 400	384	0.1158	7.7	66.5
HS 20	540	0.2288	18.0	78.7
HS 32	816	0.5228	35.0	66.9
HS 35	890	0.6207	35.0	56.4

Flow Rate = 6 grams/second (nitrogen)

Pressure = 10^{-4} torr

Temperature = 300 K

Gas Density = 1.5×10^{-7} kg/m³

Volume Rate = 3.9×10^7 liter/second

Inlet Area Minimum Required (not including loss factors) > 56 m²

Table 3. Summary of Pumping Concept Features

Parameters	Argon Prebooster	Continuous Cryogenic	ALIPP
Major components	Commercially available	Commercially available	Proven concept
Backing system	Commercially available	Commercially available	Commercially available
Special features		Radiation shields standard	High potential for pressure recovery
Gasdynamic diffuser performance	Needs demonstration	Needs demonstration	Needs demonstration
"Egg Crate" cooler performance in free molecular regime	Needs demonstration	Needs demonstration	
Areas where further work is needed	Performance and geom. and stage 1 prebooster must be demonstrated	Nature of cryogenic argon deposit must be experimentally found	Better experimental definition of plume should precede tests
	Assumed pressure ratios and stages 2 & 3 must be demonstrated	Feasibility of thermal/mechanical scraper must be demonstrated	More analysis required before meaningful tests can run

Table 4. Argon Prebooster Enhanced Vacuum System Stage Conditions
(per port)

Item	1	2	3	OVB	Roots Blower
Driver Press (torr)	0.3	3.0	8.4	-	-
Throat Dia/Width (inch)	0.065	2.55	2.0	-	-
Exit Dia/Width (inch)	3.1	24.0	11.0	-	-
Inlet Press (torr)	3×10^{-4}	1.5×10^{-3}	8.4×10^{-3}	4.6×10^{-2}	2.0
Outlet Press (torr)	1.5×10^{-3}	8.4×10^{-3}	4.6×10^{-2}	2.0	50.0
Inlet Temperature (°R)	300	142	92	82	Amb.
Outlet Temperature (°R)	142	92	82	Amb.	Amb.
Inlet Volume Rate (ft ³ /s)	15,300	4,100	1,200	400	60
Outlet Volume Rate (ft ³ /s)	4,100	1,200	400	60	2

Table 5. Summary of Advanced Pumping System Costs

<u>Concept</u>	<u>Estimated R&D^a</u>	<u>Engineering Fab. & Install.</u>	<u>(Major) Acquisition</u>	<u>Building and Common Features</u>	<u>Totals</u>
Argon Prebooster, etc.	\$1300K	\$1202K	\$1400K	\$1612K ^b	\$6014K
Continuous Cryogenic	\$1300K	\$974K	\$586K	\$1612K	\$4472K
ALIPP	\$1686K	\$985K	\$600K	\$1612K	\$4883K

^aIncludes diffuser development cost for all concepts.

^bCommon cost of \$1362K plus \$250K for Building cost.

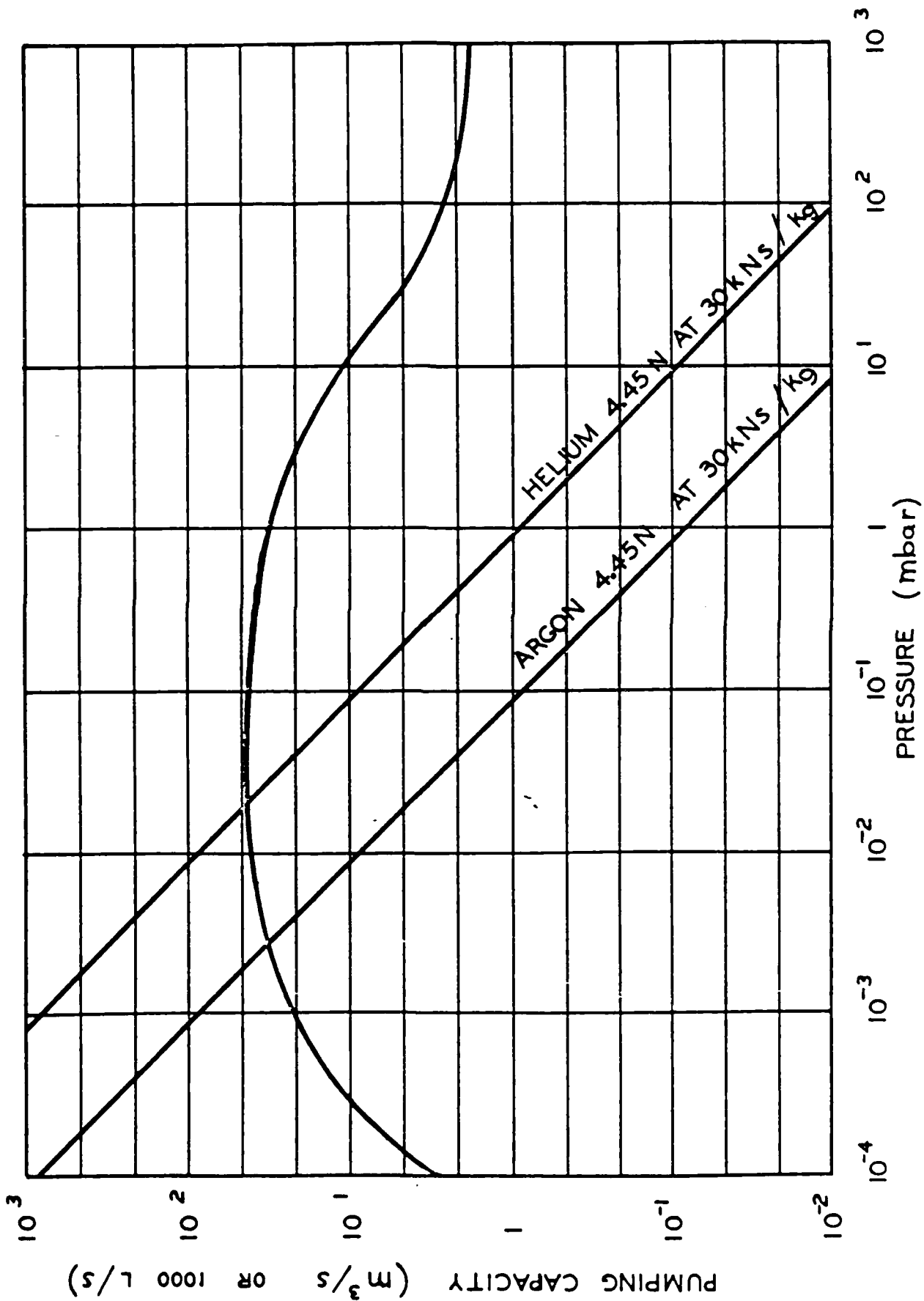


FIGURE 1 STUTTGART FACILITY VACUUM CAPABILITY

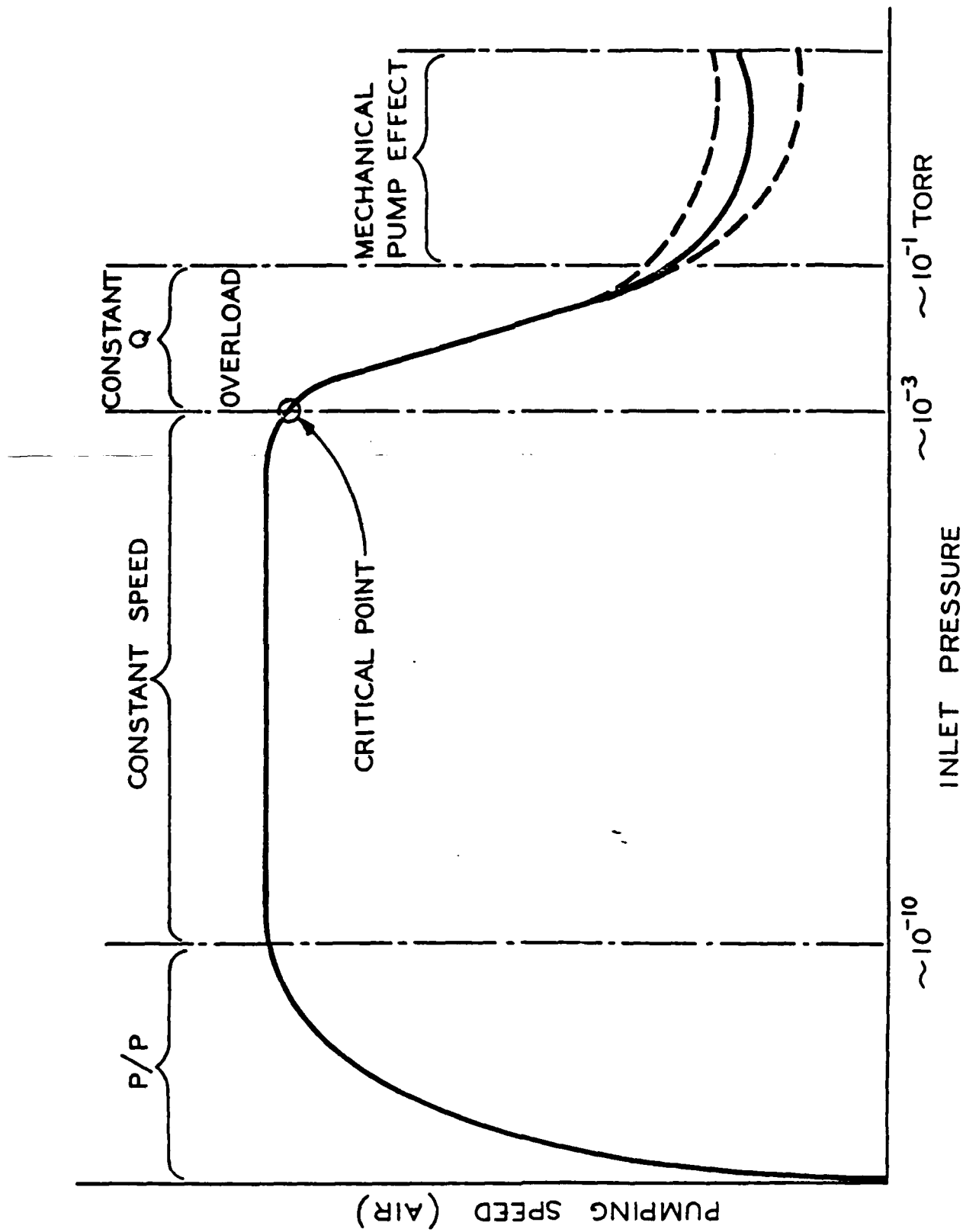


FIGURE 2 DIFFUSION PUMP OPERATING REGIME

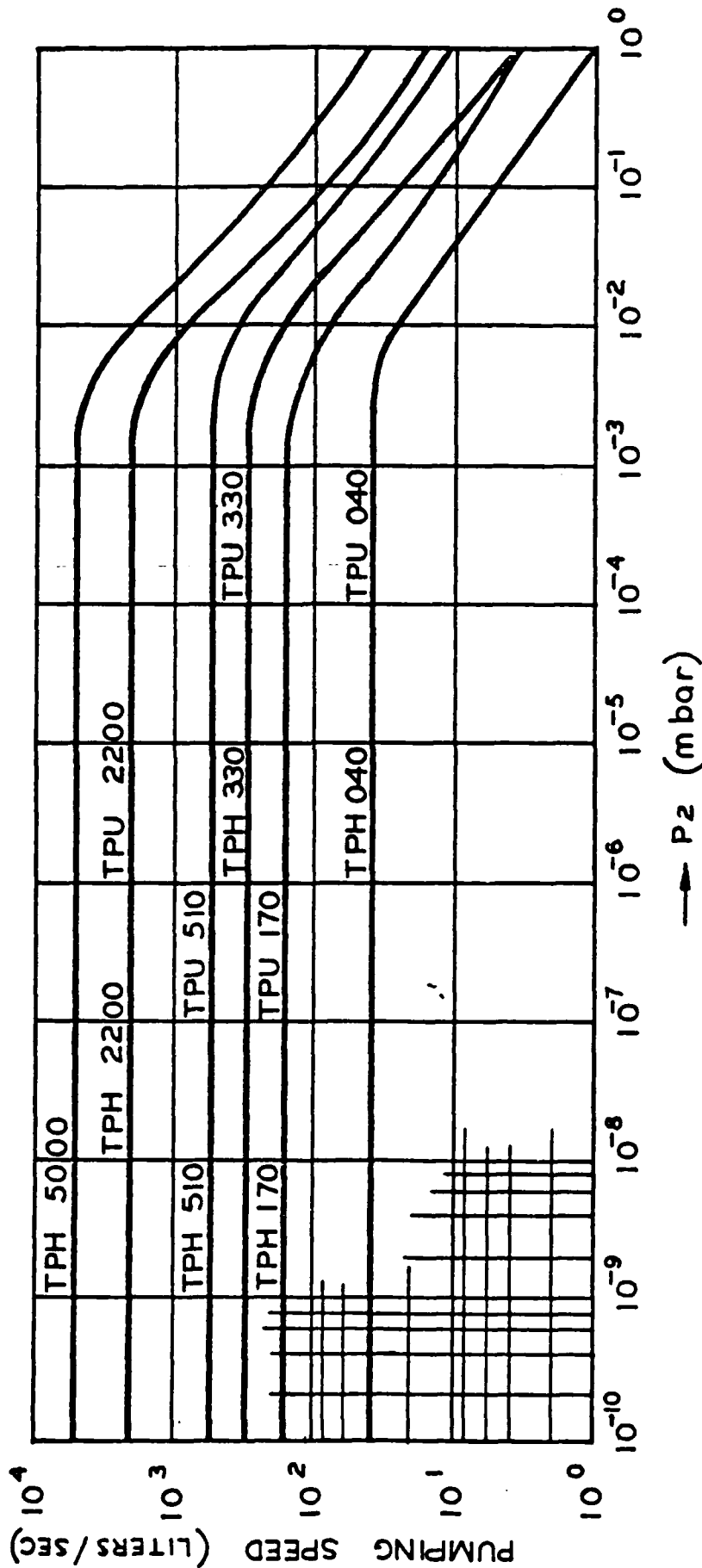


FIGURE 3 TYPICAL PUMPING CHARACTERISTIC CURVES
FOR TURBOMOLECULAR PUMP

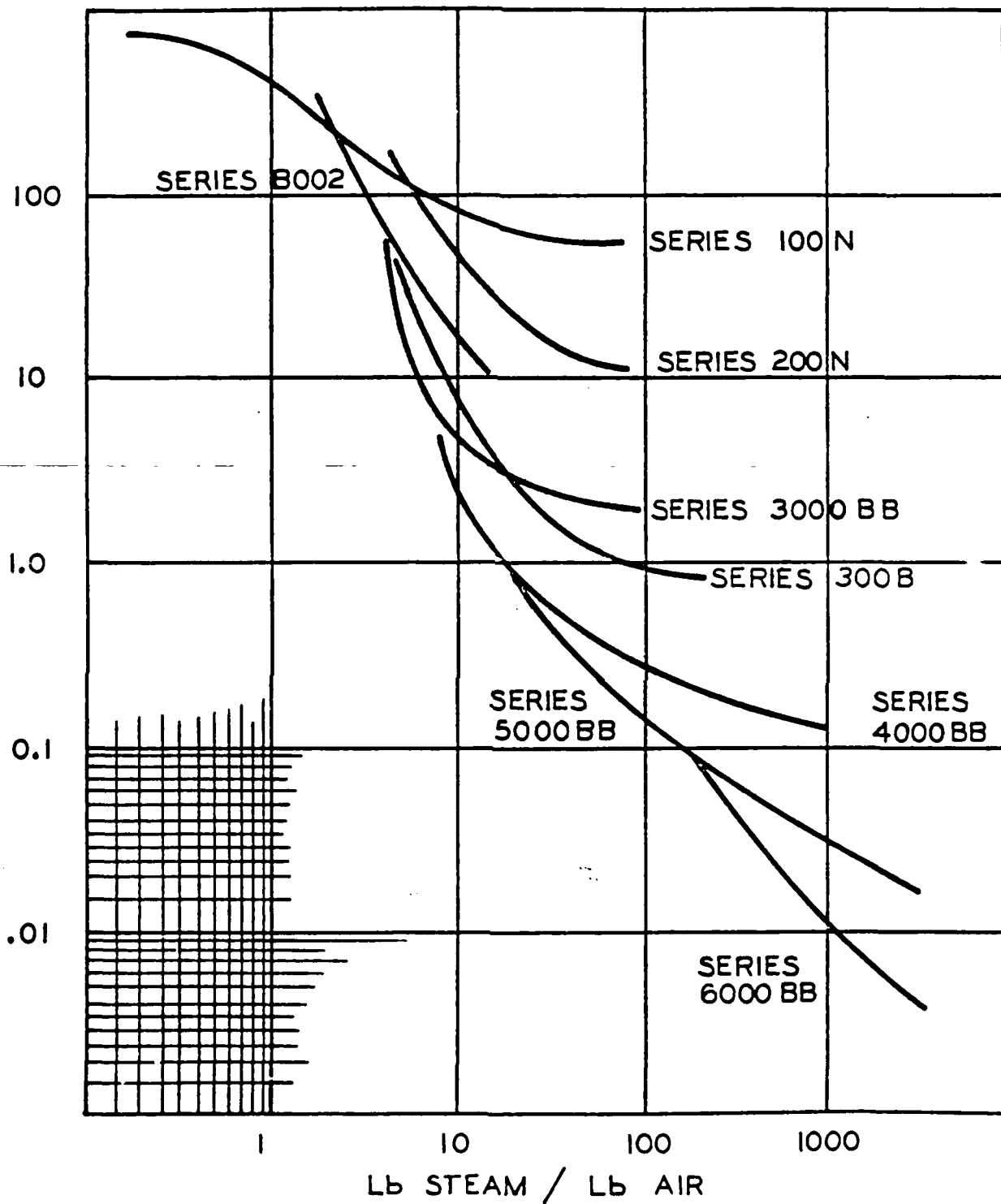


FIGURE 4 TYPICAL PRESSURE VS STEAM-TO-GAS MASS FLOW RATIOS FOR STEAM EJECTORS

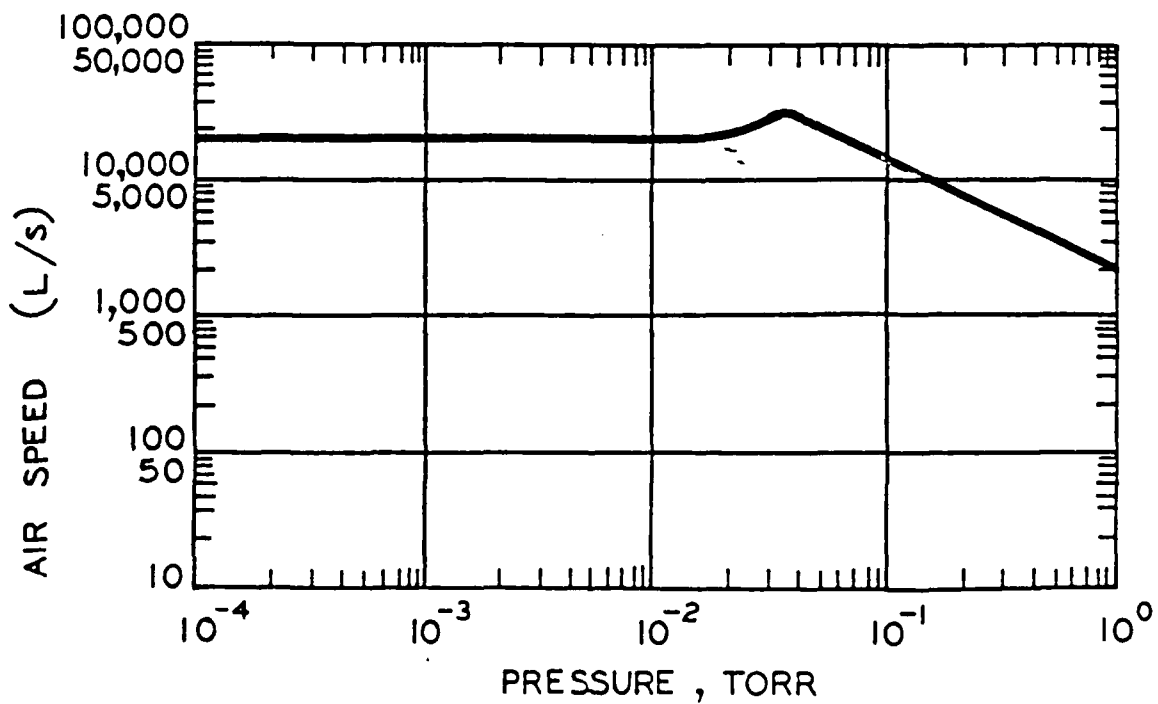
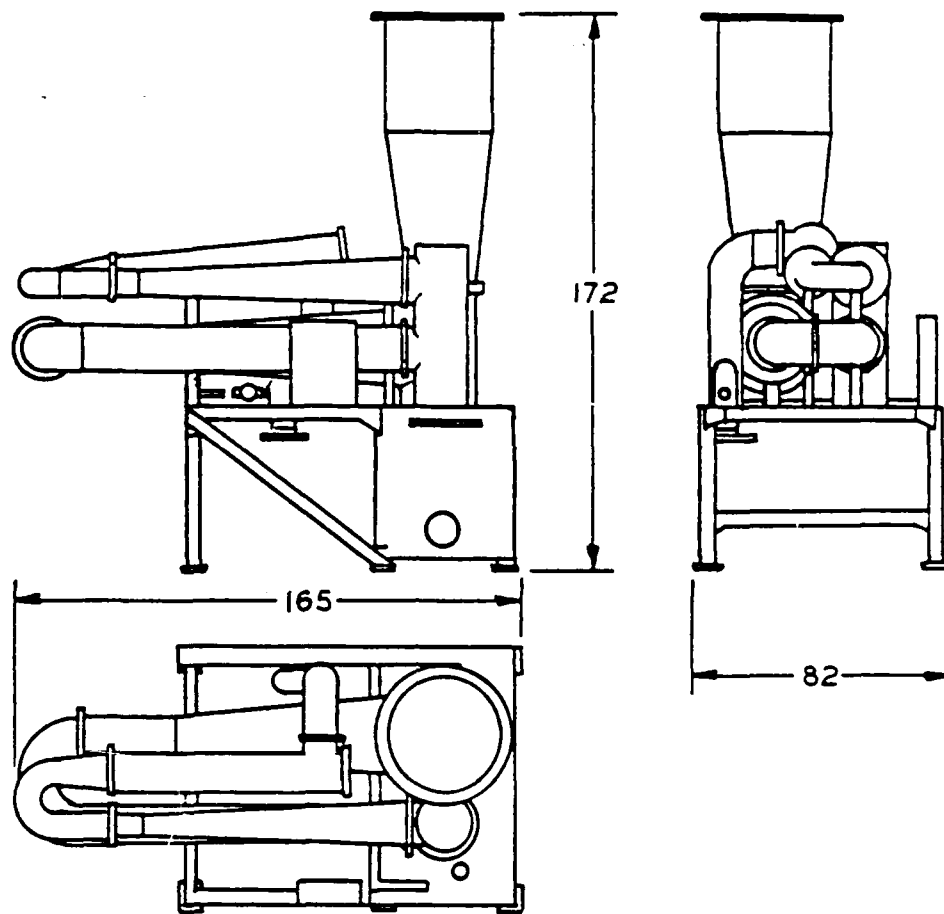


FIGURE 5

OIL VAPOR BOOSTER PUMP WITH
TYPICAL CHARACTERISTIC CURVE

STAGE 1

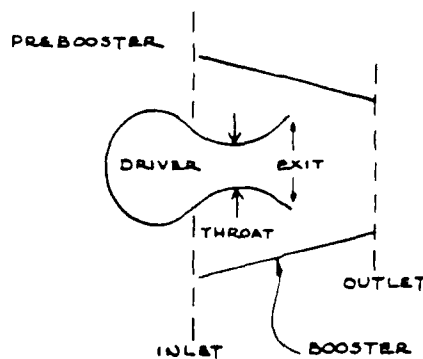
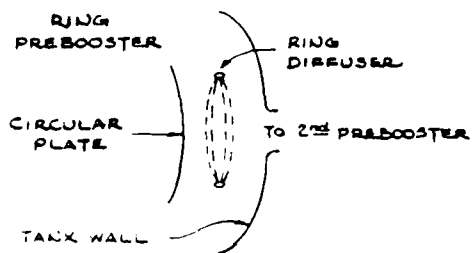
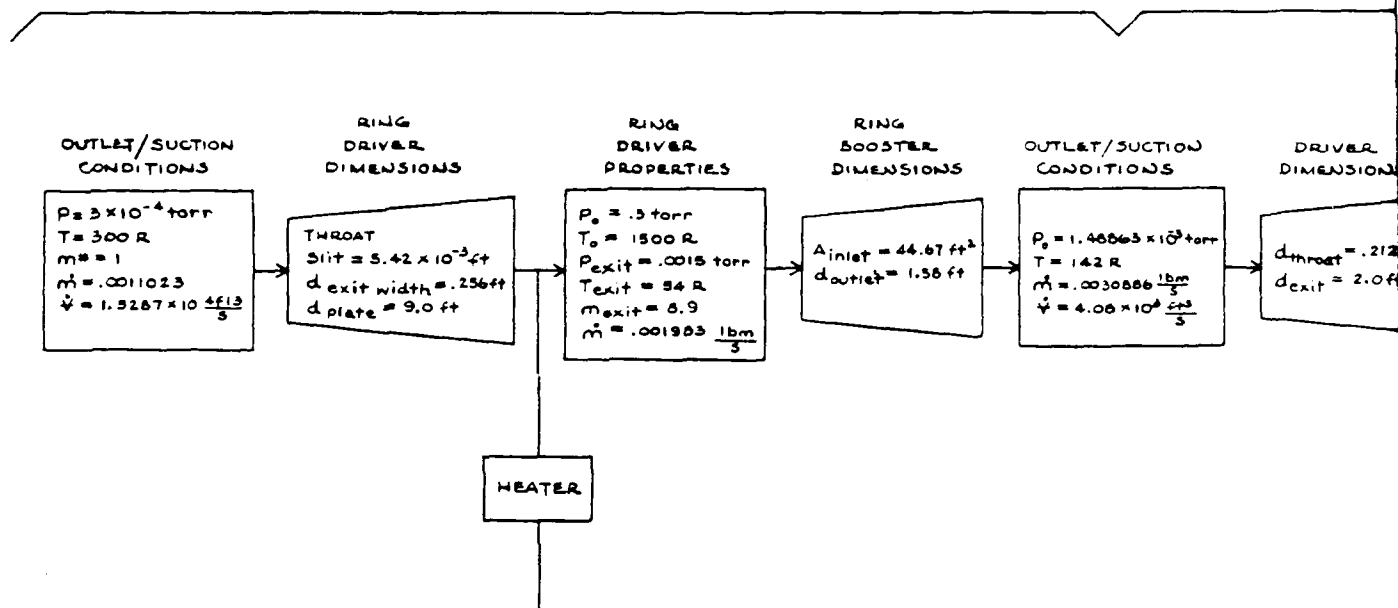


Figure 6. Argon Pr

STAGE 1

STAGE 2

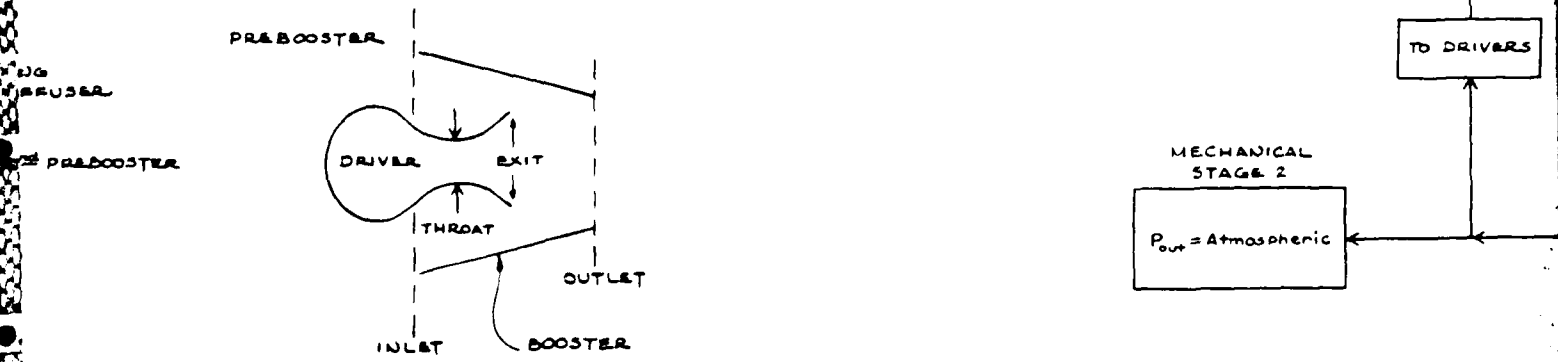
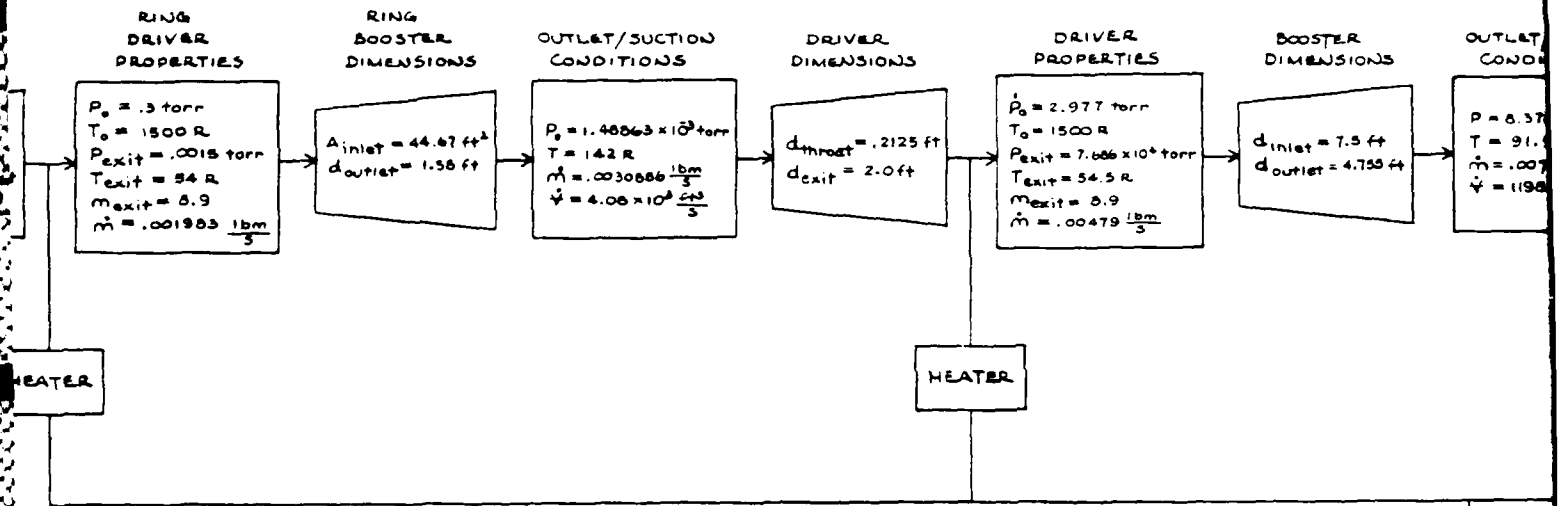
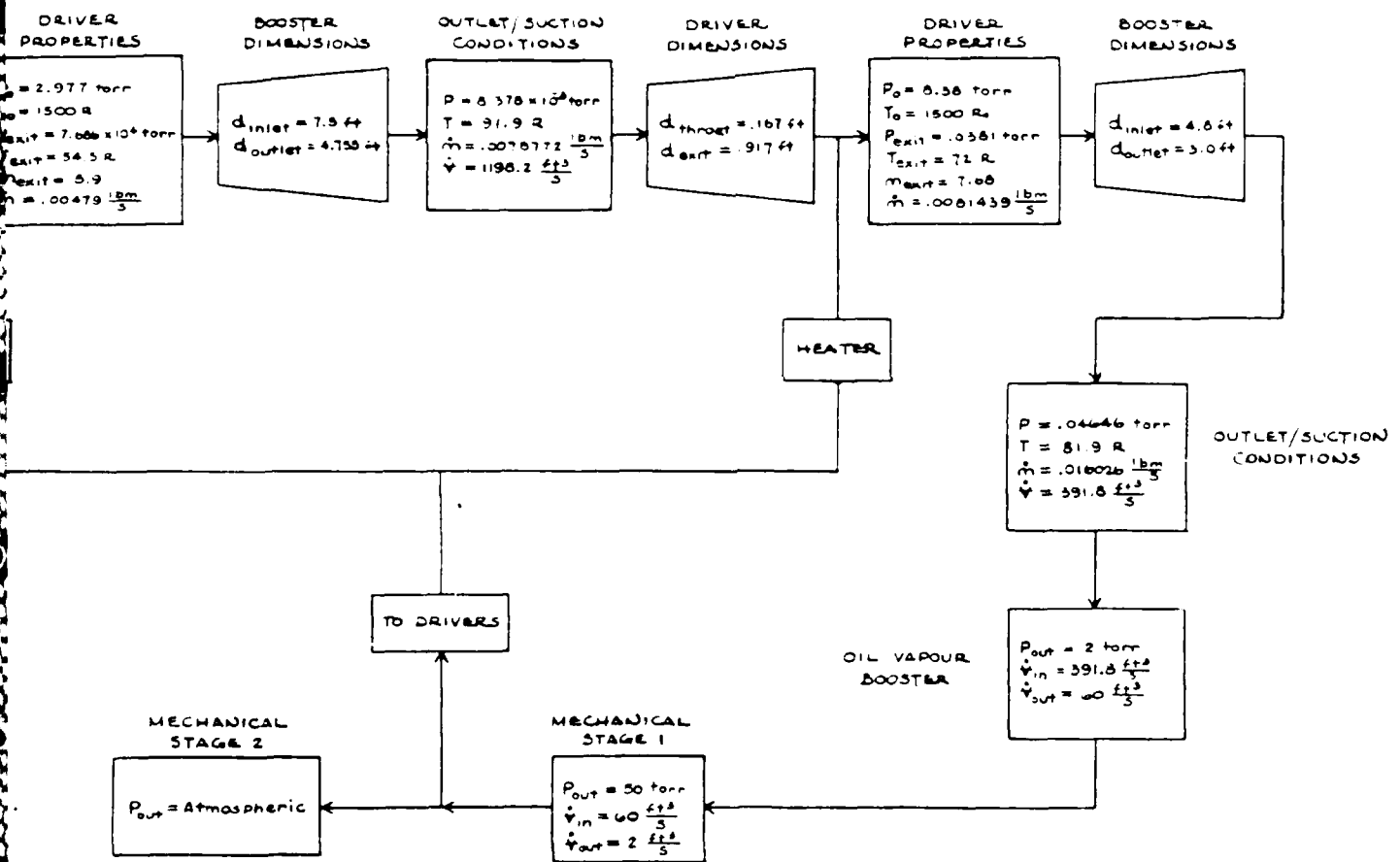


Figure 6. Argon Prebooster Block Diagram

STAGE 2

STAGE 3



er Block Diagram

343

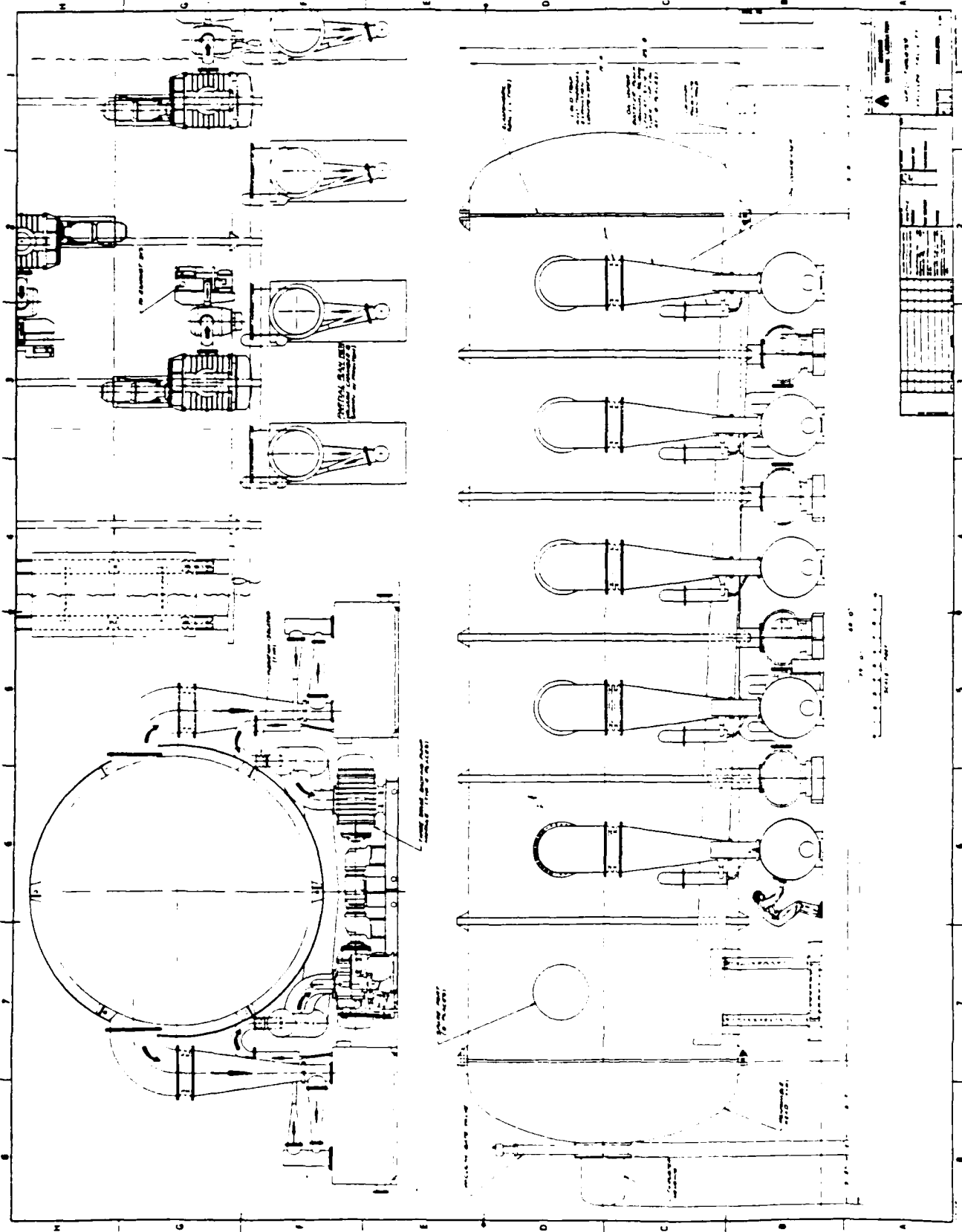


FIGURE 7 OIL VAPOR BOOSTER PUMPING SYSTEM ARRANGEMENT

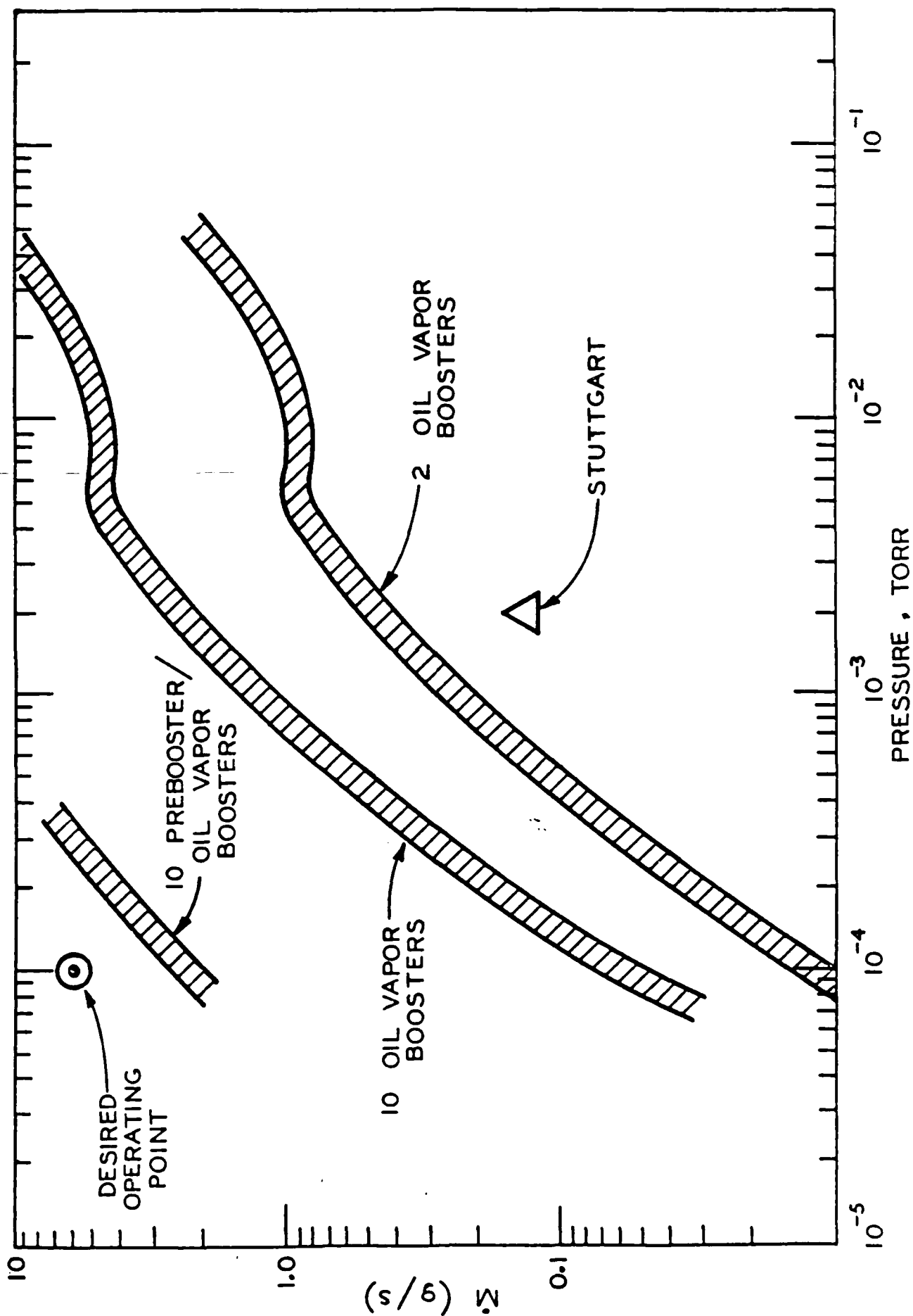


FIGURE 8 OPERATING CURVES OF STEADY STATE FACILITIES

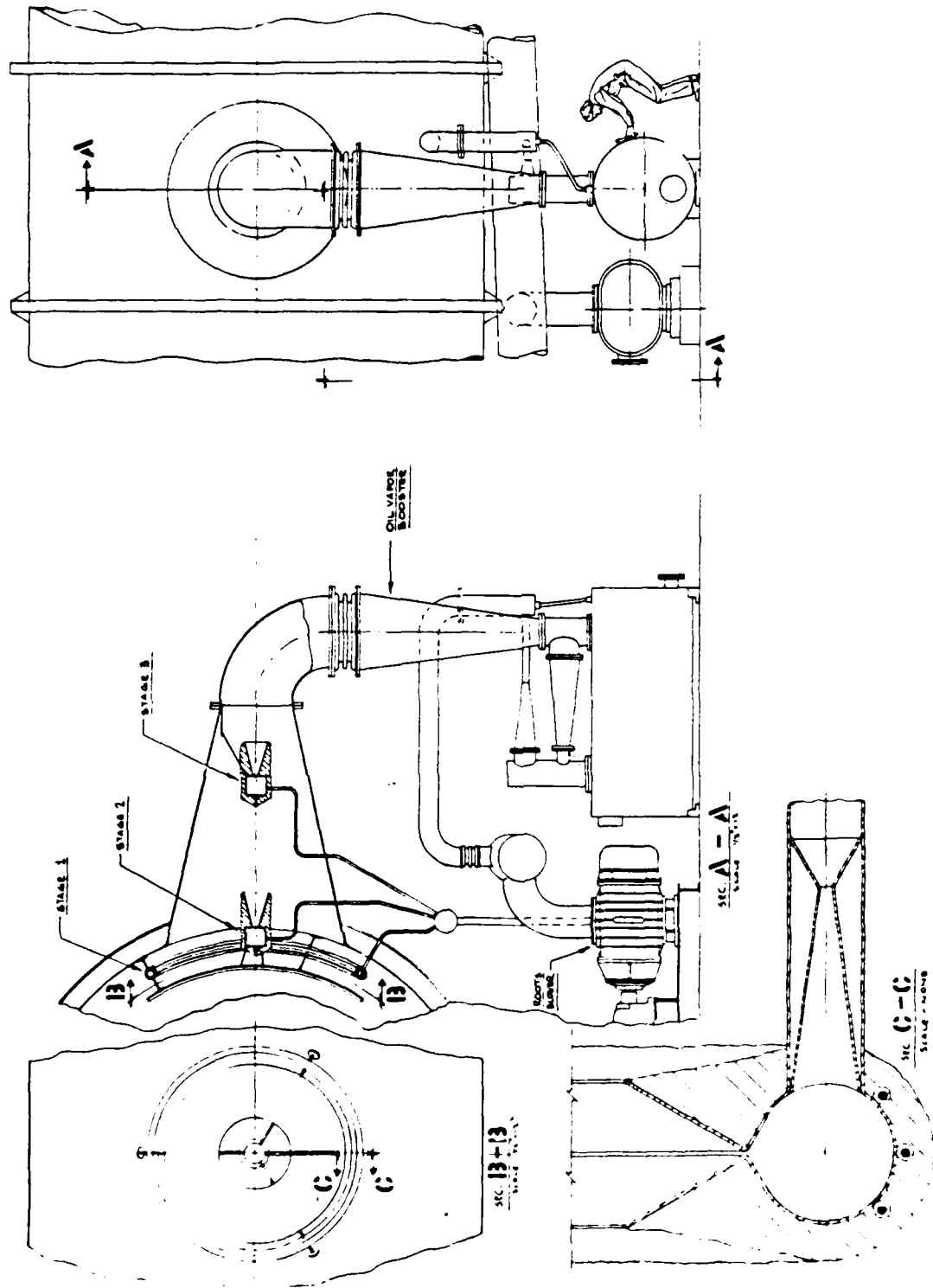


FIGURE 9 ARGON PRE-BOOSTER FITTED TO VACUUM CHAMBER

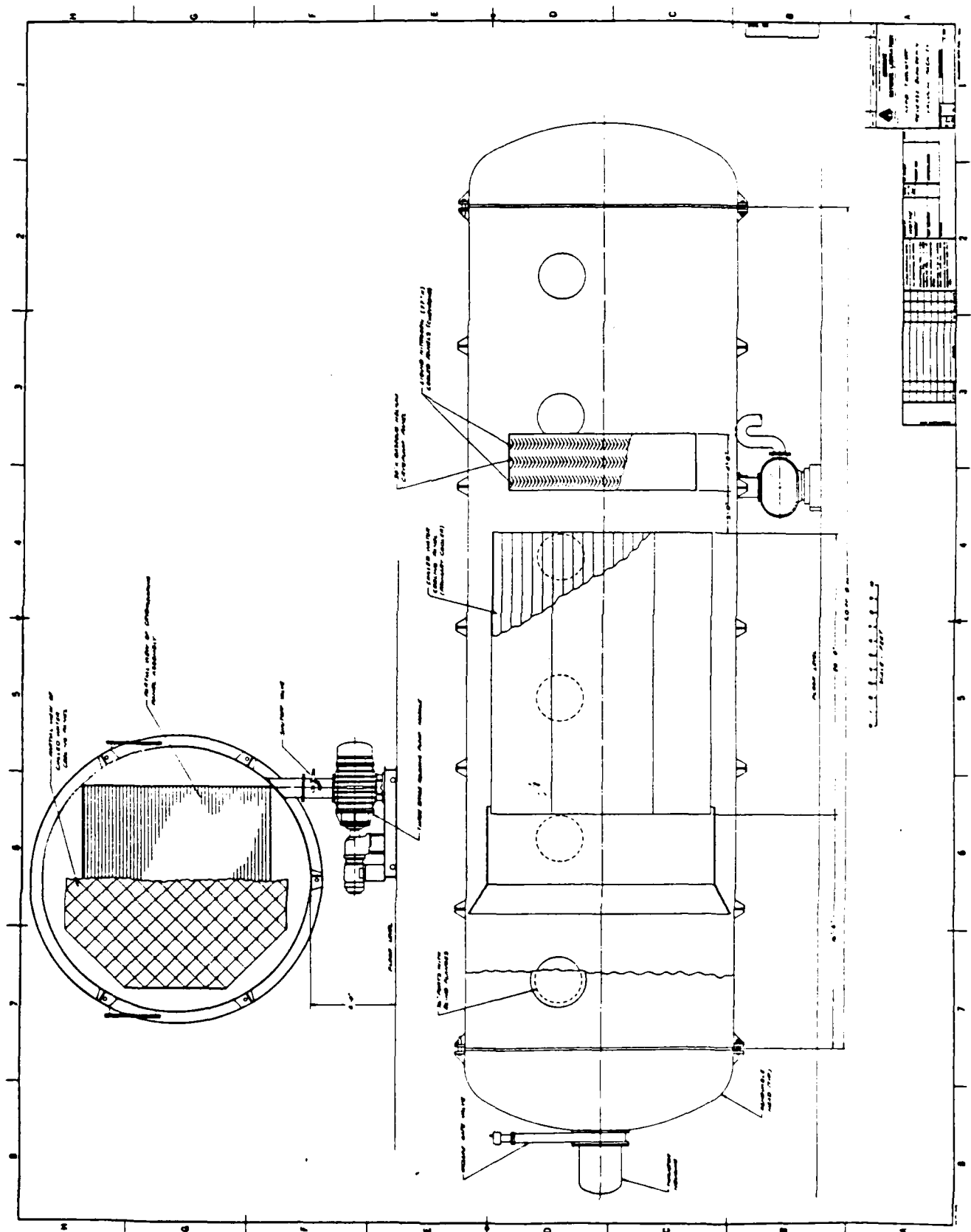


FIGURE 10 CONVENTIONAL CRYOPUMPING ARRANGEMENT

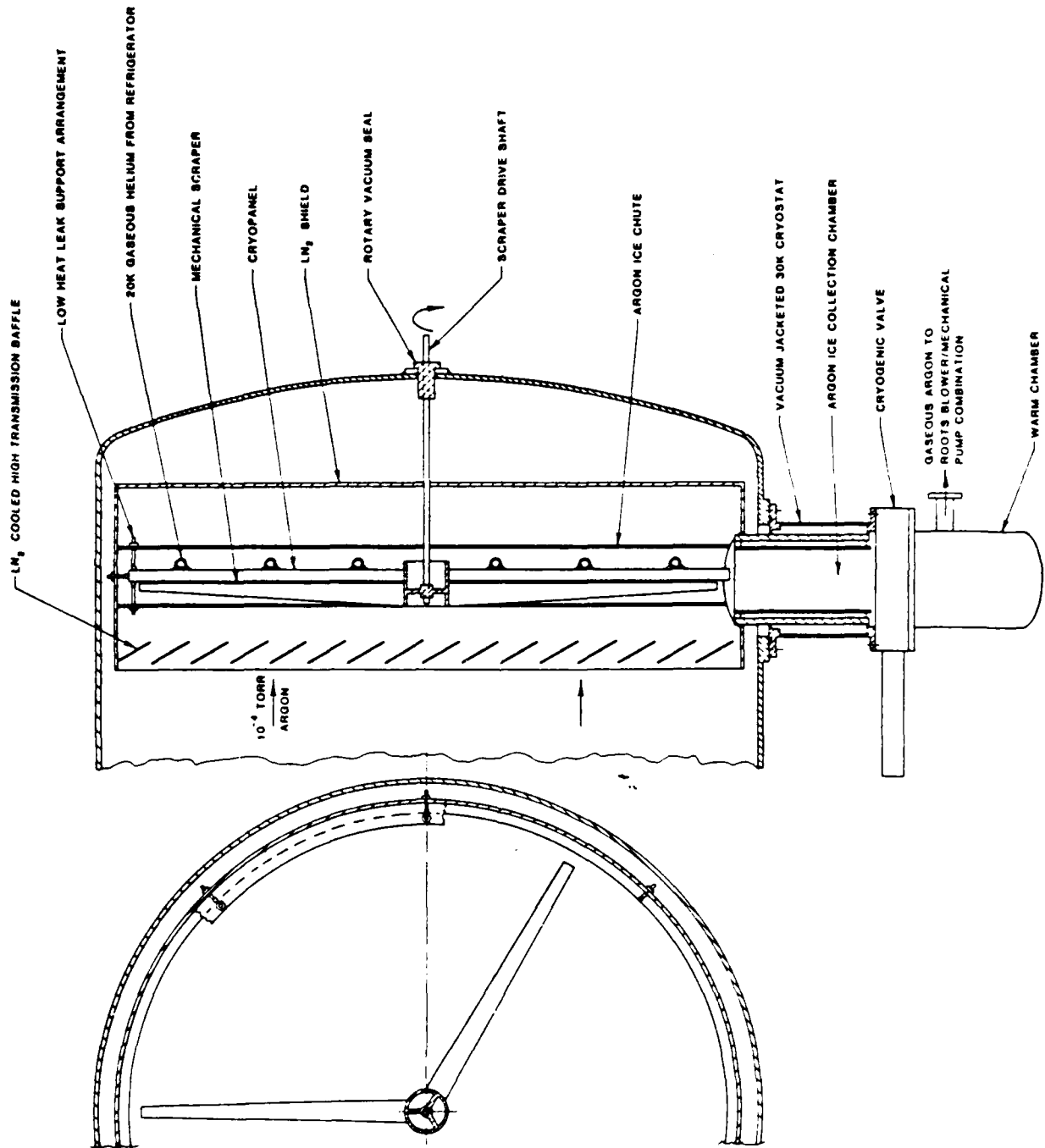


FIGURE 11 CONTINUOUS CRYOPUMPING SYSTEM WITH MECHANICAL SCRAPER

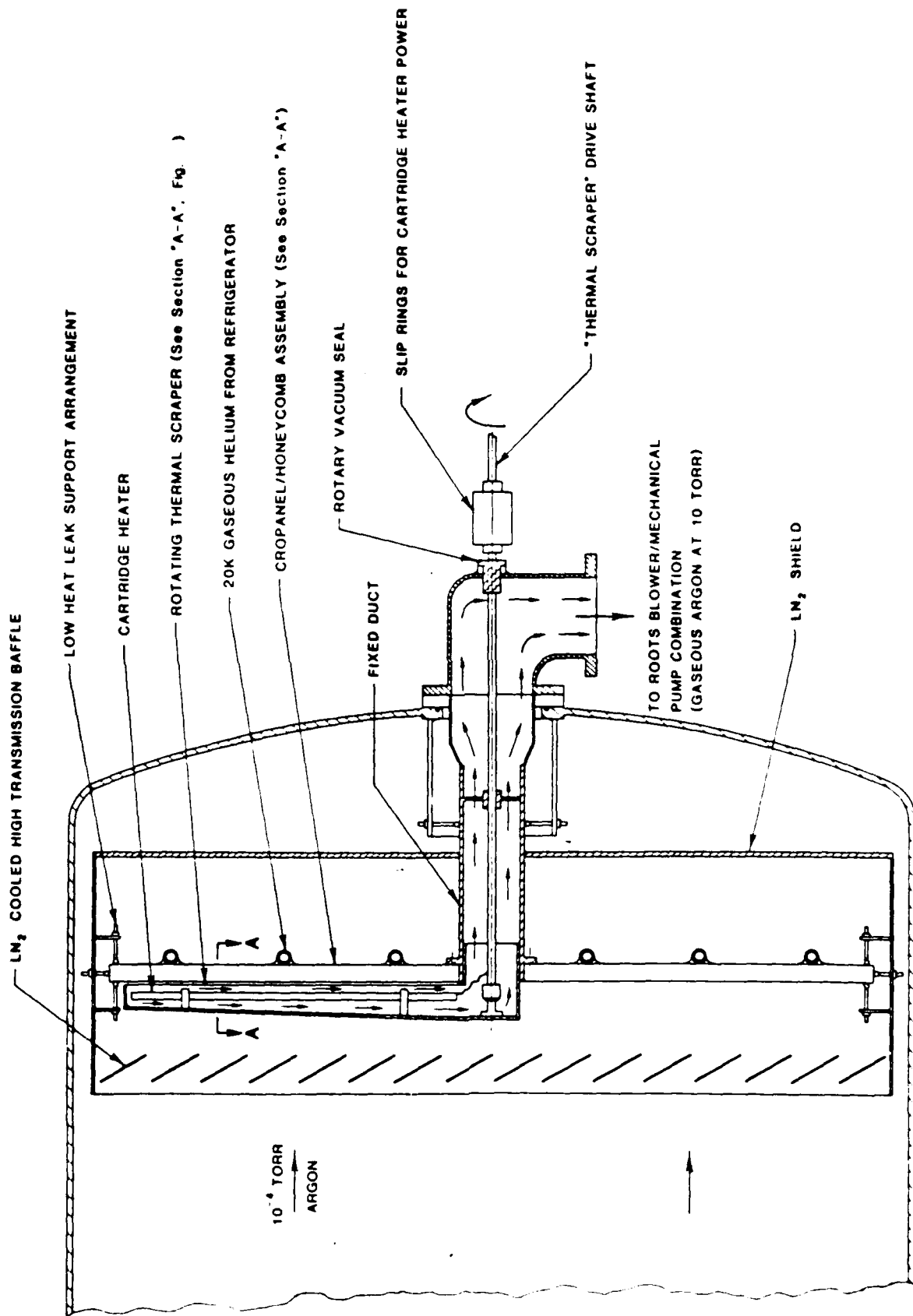
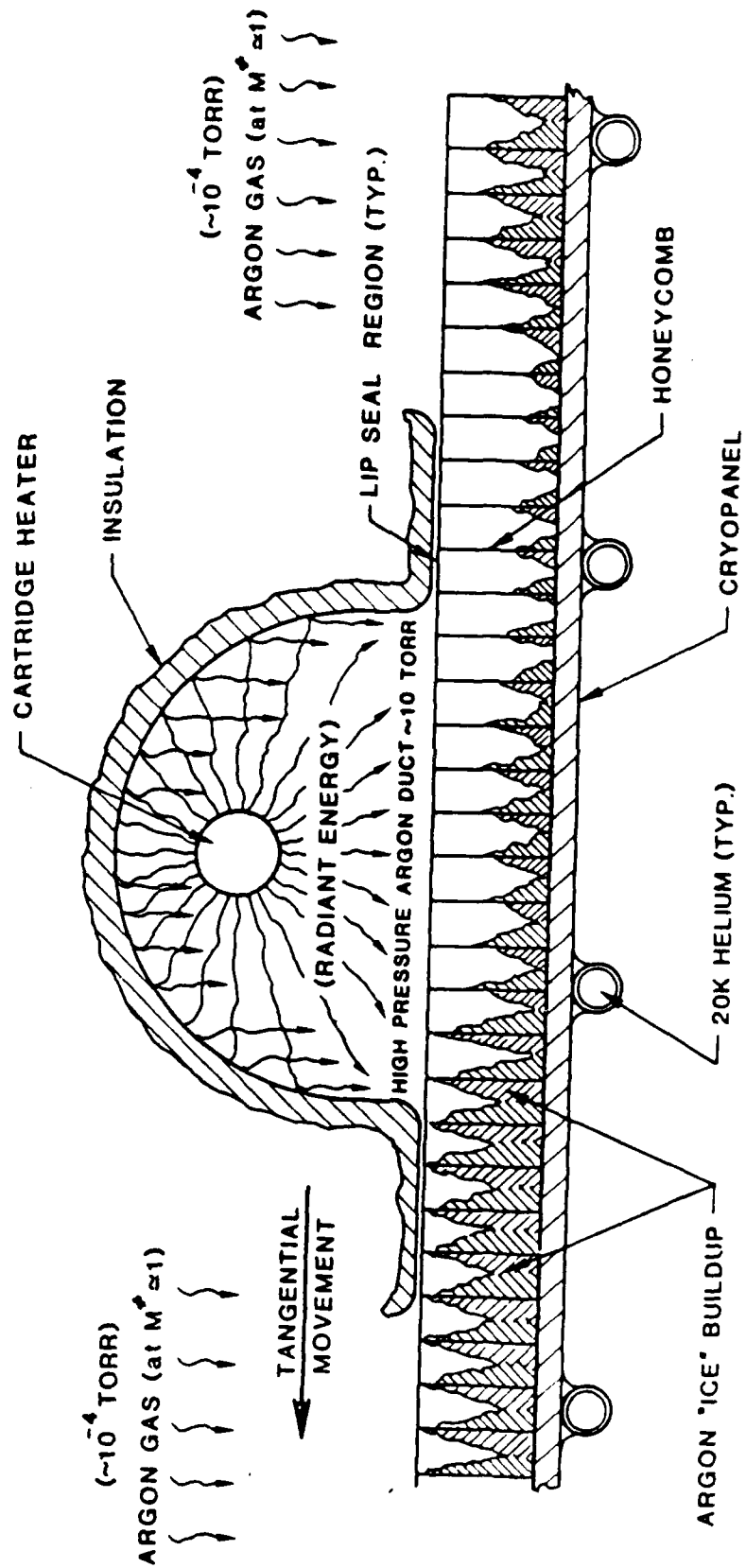


FIGURE 12 CONTINUOUS CRYOPUMPING SYSTEM WITH THERMAL SCRAPER



SECTION A - A

FIGURE 13 THERMAL SCRAPER CROSS-SECTION

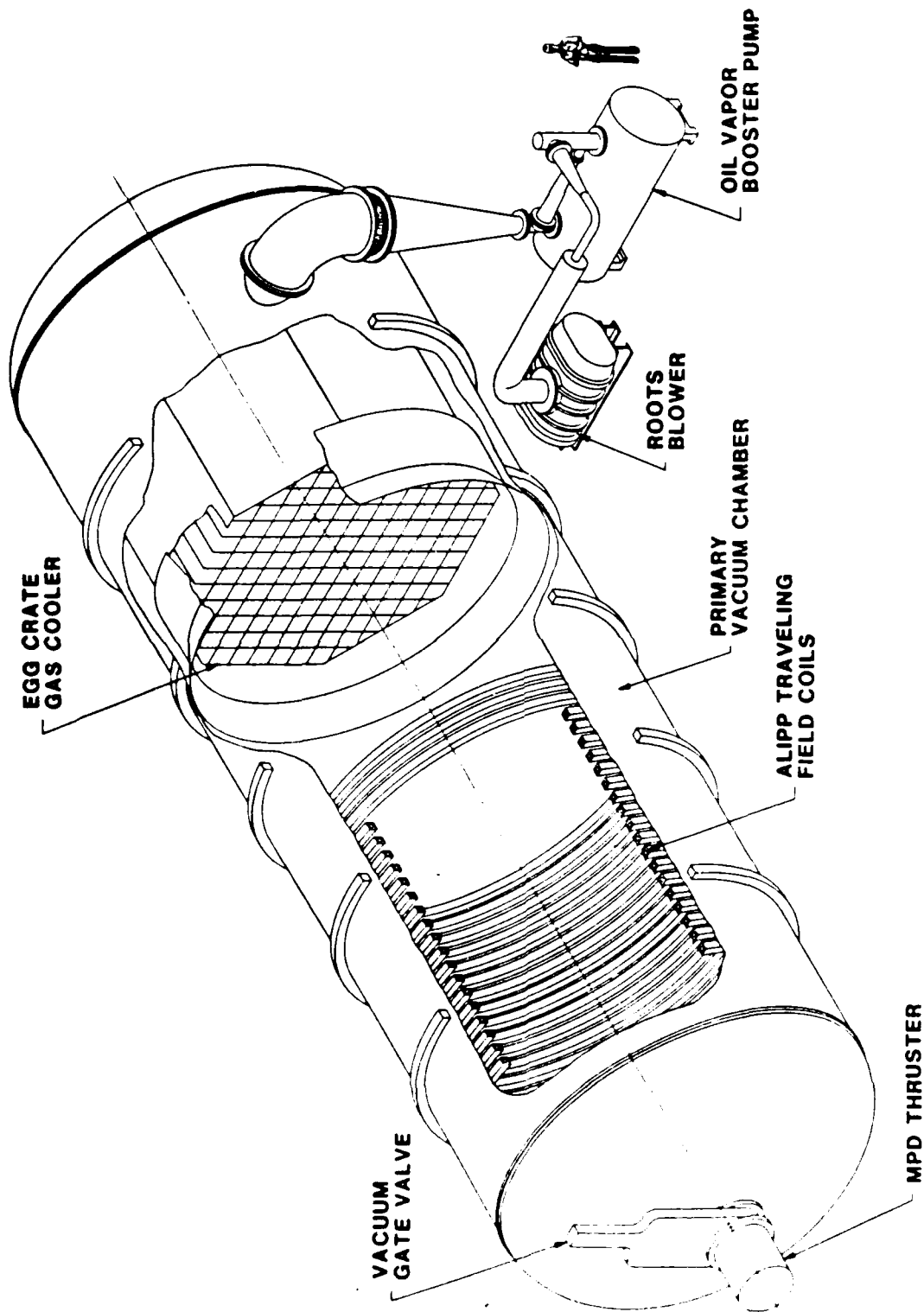


FIGURE 14 AXISYMMETRIC LINEAR INDUCTION PLASMA PUMP (ALIPP)

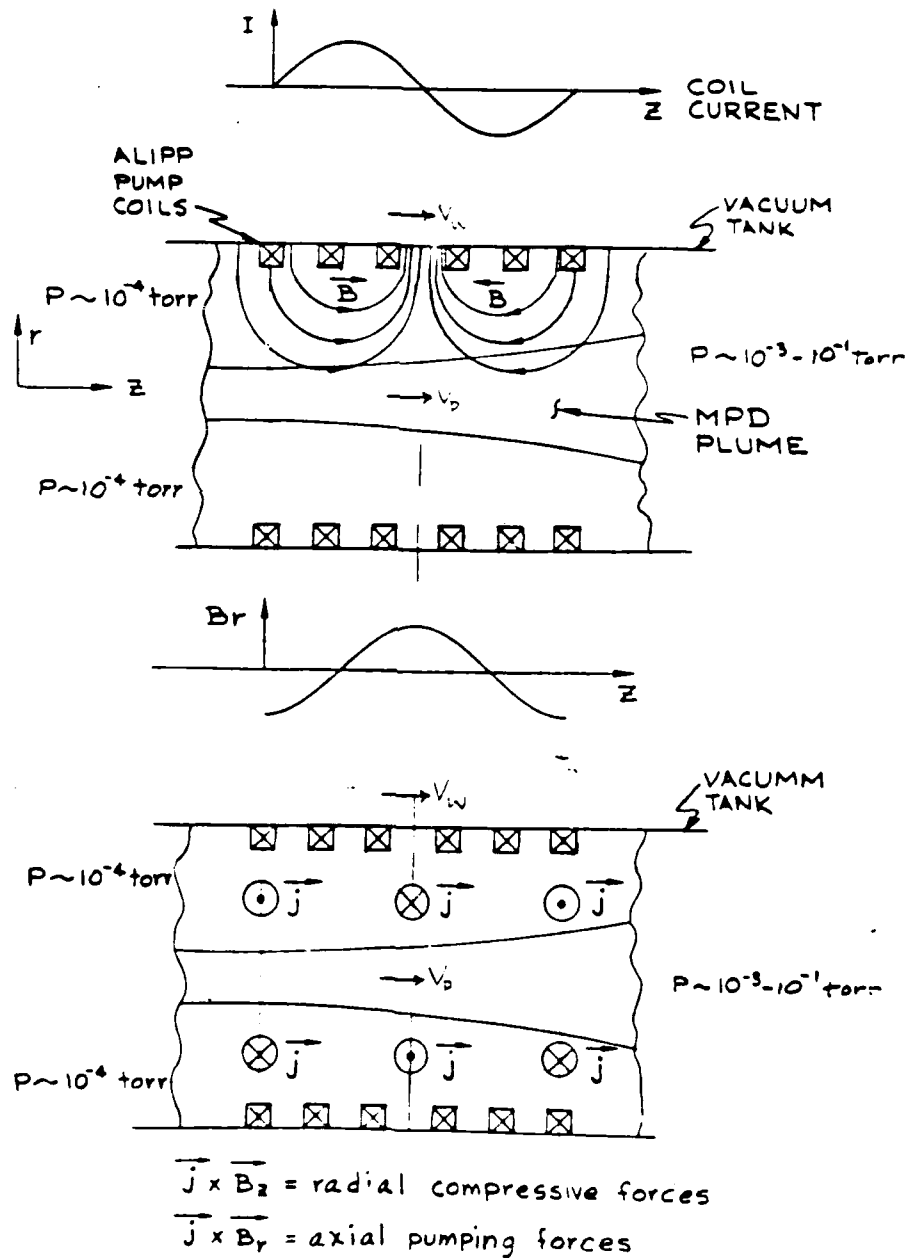


FIGURE 15 OPERATING PRINCIPLE OF AXISYMMETRIC LINEAR INDUCTION PLASMA PUMP (ALIPP)

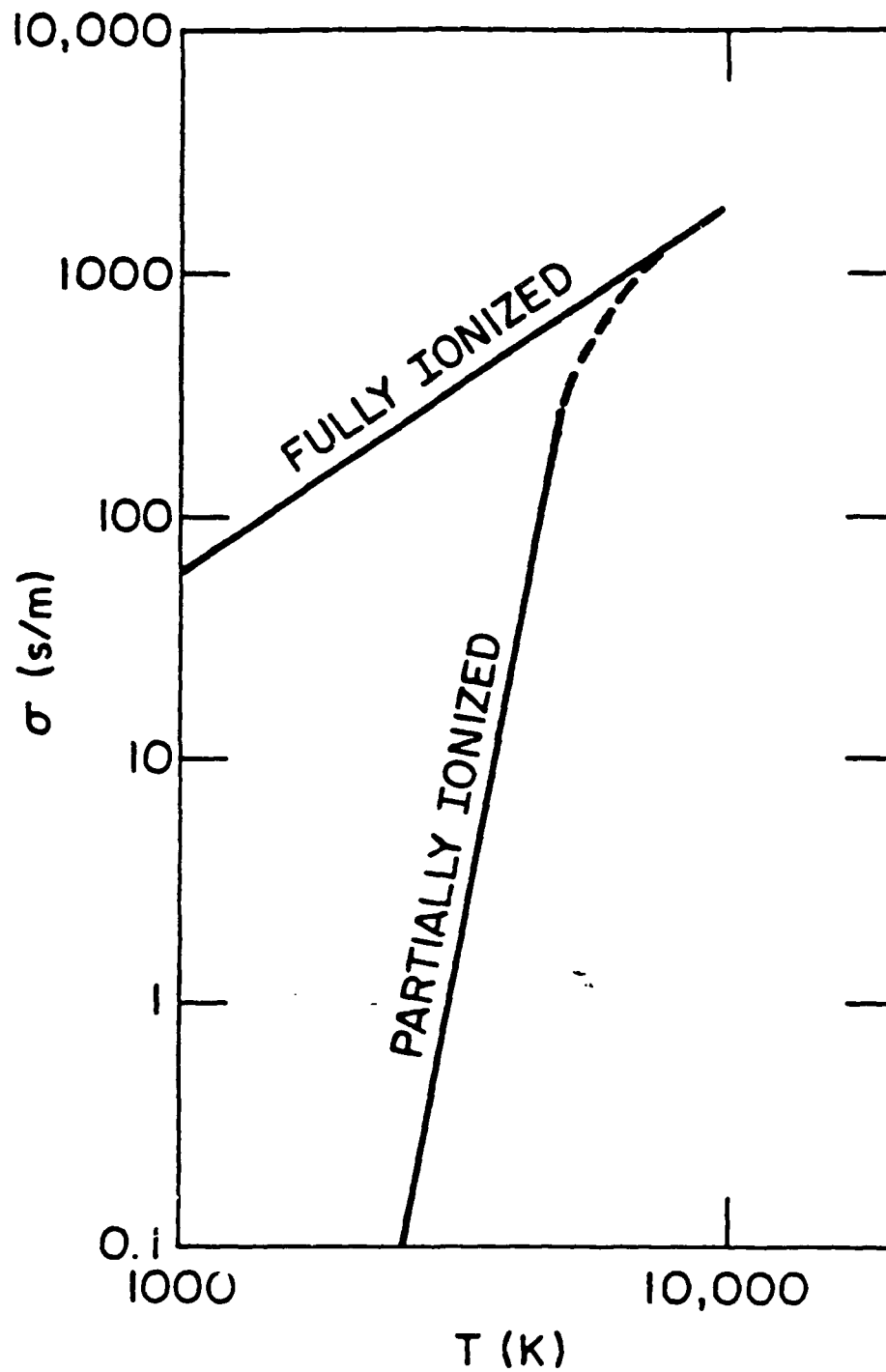


FIGURE 16 CONDUCTIVITY OF ARGON

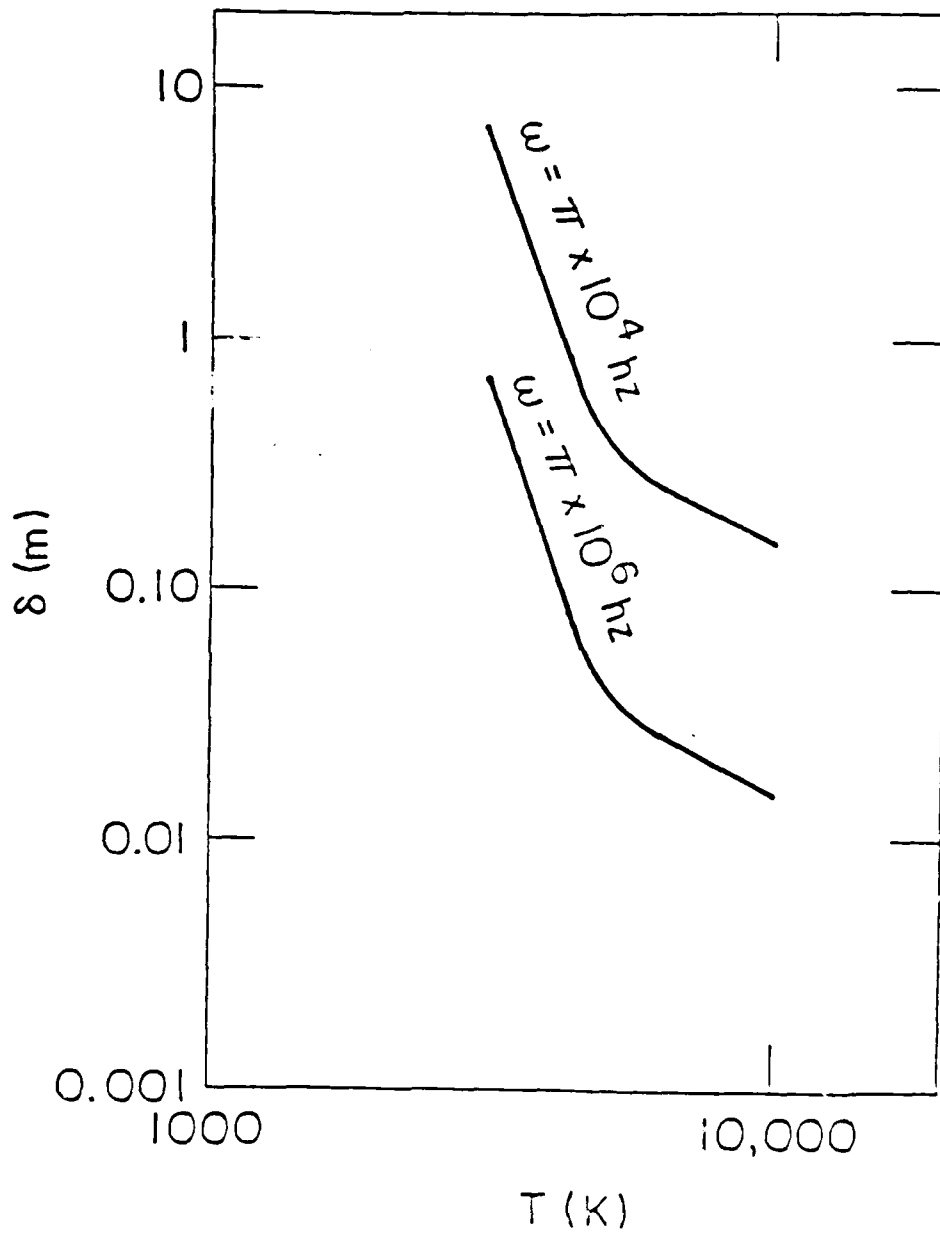


FIGURE 17. ALIPP SKIN DEPTH

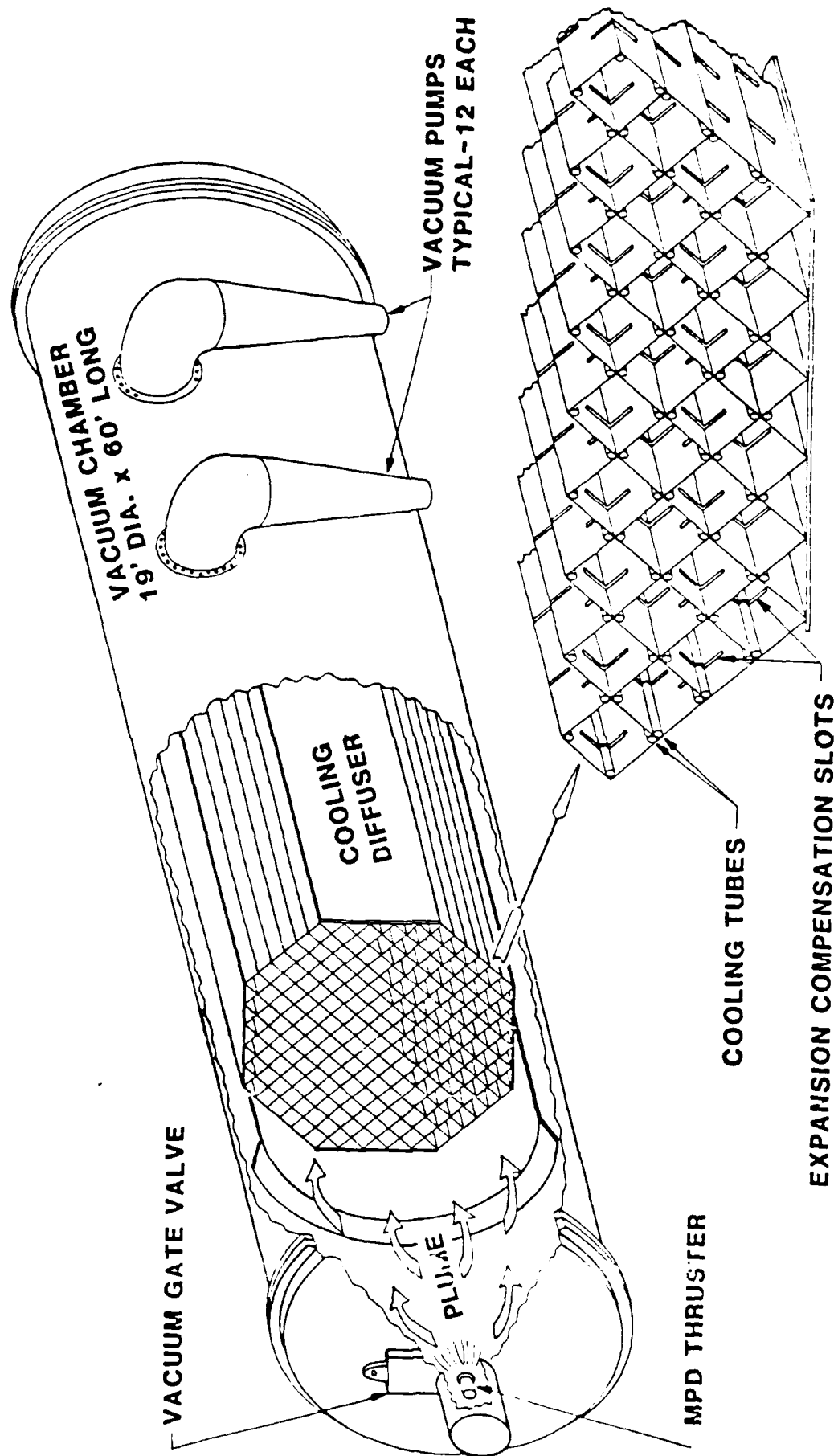


FIGURE 18. MPD THRUSTER VACUUM SYSTEM WITH INTERNAL COOLING DIFFUSER

APPENDIX

DESIGN CALCULATIONS FOR ARGON PREBOOSTER

DESIGN CALCULATIONS FOR ARGON PREBOOSTER

1. Volume Flow Rate of Argon at 6 gm/s and 10^{-4} Torr.

Given: $\dot{W} = 6$ gm/s (0.013223 lbm/s)

$p = 10^{-4}$ Torr (1.9342×10^{-6} lbf/in²)

MW = 40

$R_0 =$ universal gas constant = $1545 \frac{\text{ft lbf}}{\text{lbm } ^\circ\text{R}}$

$T_1 = 150$ °R (83K cryocooled temp.)

$T_2 = 300$ °R (166K near ambient temp.)

To calculate = $\dot{V}_{150^\circ\text{R}}$ and $\dot{V}_{300^\circ\text{R}}$

$$\text{Equation: } \rho = \frac{p}{(R_0/\text{MW})T} \quad (\text{A-1})$$

and

$$\dot{V} = W/\rho \quad (\text{A-2})$$

Applying Eqs. (1) and (2), we get

$$\rho_{150^\circ\text{R}} = 4.8073 \times 10^{-3} \text{ lbm/ft}^3$$

$$\rho_{300^\circ\text{R}} = 2.4037 \times 10^{-8} \text{ lbm/ft}^3$$

$$\dot{V}_{150^\circ\text{R}} = 2.7516 \times 10^5 \text{ ft}^3/\text{s}$$

$$\dot{V}_{300^\circ\text{R}} = 5.5033 \times 10^5 \text{ ft}^3/\text{s}$$

The results calculated at a temperature of 300 °R will be adopted because this temperature is believed to be more realistic.

2. Number of Oil Vapor Booster Pumps Required

(2.1) The oil vapor booster pump of Edwards High Vacuum CVC Inc., operates on the vapor ejection principle and has a pumping speed of 22,000 liter/s or 776.9 ft³/s. (See Fig. A-1)

Thus, number of oil booster pumps required assuming operating at near ambient temperature of 300 °R is $5.5033 \times 10^5 \div 776.9 \approx 720$ units. This value is unacceptable.

(2.2) The inlet diameter of this pump is 3 ft. Thus, the inlet velocity is $776.9 \text{ ft}^3/\text{s} \div (\pi 3^2/4) \text{ ft}^2$ or 109.91 ft/s .

The speed of sound at $300 \text{ }^\circ\text{R}$ is

$$\left[\left(\frac{2\gamma}{\gamma+1} \right) g_c \left(\frac{R}{MW} \right) T \right]^{1/2} = 683.19 \text{ ft/s,}$$

$$\therefore M\# = \frac{109.91}{683.19} = 0.1609.$$

This result indicates that this pump ordinarily operates at volume flow rates significantly lower than choked (sonic) flow.

3. Calculations of 1st Stage Prebooster Ejector

(3.1) Calculated results from 2.1 and 2.2 show that an unacceptable number (720 units) of oil vapor booster pumps are required to handle a flow of Argon at 6 gm/s and 10^{-4} Torr . Therefore preboosters are needed to boost Argon gas from 10^{-4} Torr to an inlet pressure that is commensurate with the capacity of oil vapor boosters. In the following calculations, the vacuum chamber is assumed to have 12 ports for installing this prebooster system.

Assuming that with an Argon "ejector" as a prebooster we can draw at $M\# = 1$ at a pressure of 10^{-4} Torr and a temperature of $300 \text{ }^\circ\text{R}$, the required volume flow rate per port is given by

$$550,330 \text{ ft}^3/\text{s} \div 12 = 45,861 \text{ ft}^3/\text{s.}$$

at

$$M\# = 1, U = 683.19 \text{ ft/s.}$$

∴ The cross-sectional area per port

$$= 45861 \text{ ft}^3 \div 683.19 \text{ ft/s}$$

$$= 67.13 \text{ ft}^2$$

or the port diameter

$$= (67.13 \times 4/\pi)^{0.5} \text{ ft}$$

$$= 9.244 \text{ ft}$$

This value is too big.

In order that the port diameter is of reasonable size, the suction pressure needs to be increased. Assuming that the suction pressure is now 3×10^{-4} Torr, with a mass flow rate of 6 gm/s, and temperature of 300 °R, the volume flow rate is

$$\dot{V} \text{ at } 3 \times 10^{-4} \text{ Torr, } 300 \text{ °R} = 1.8344 \times 10^5 \text{ ft}^3/\text{s}$$

$$\dot{V} \text{ per port} = 1.5287 \times 10^4 \text{ ft}^3/\text{s}$$

The cross-sectional area per port

$$= 1.5287 \times 10^4 \text{ ft}^3/\text{s} \div 683.19 \text{ ft/s}$$

$$= 22.376 \text{ ft}^2$$

or, the port diameter

$$= (22.376 \times 4/\pi)^{0.5} \text{ ft}$$

$$= 5.338 \text{ ft (64 inches)}$$

The mass flow rate of Argon through each port, \dot{W}_{suction}

$$= 0.013228 \text{ lbm/s} \div 12$$

$$= 0.0011023 \text{ lbm/s}$$

(3.2) Calculations of the ejector parameters that will enable the boosting of Argon gas from an inlet pressure of 3×10^{-4} Torr to the operating conditions commensurate with the capacity of an oil vapor booster.

Employing the standard ejector program (Ref. 12), calculations were performed with results shown in Table A-1, where

$$PR \text{ (Pressure ratio)} = \frac{P_{\text{suction}}}{P_{\text{driver}}} \text{ or } \frac{P_{\text{ob}}}{P_{\text{oa}}}$$

$$AR \text{ (area ratio)} = \frac{A_{\text{mixer (ejector throat)}}}{A_{\text{driver throat}}}$$

and

$$TR \text{ (temperature ratio)} = \frac{T_{\text{driver}}}{T_{\text{suction}}}$$

The locations of these and other suction parameters are illustrated in a schematic of an ejector shown in Fig. A-2.

Case A

$$\text{Choose } PR = 0.001,$$

$$AR = 300,$$

and

$$TR = 5,$$

then

$$P_{\text{driver}} = P_{\text{oa}} = 0.3 \text{ Torr},$$

$$T_{\text{driver}} = 1500 \text{ }^\circ\text{R},$$

and from the ejector optimization program,

$$\dot{W}_b/\dot{W}_a = \dot{W}_{\text{suction}} / \dot{W}_{\text{driver}} = 0.600426,$$

and

$$P_3/P_{\text{ob}} = P_{\text{ejector outlet}} / P_{\text{suction}} = 5.46617$$

Assuming a 90% efficiency, the "actual"

$$\dot{W}_b/\dot{W}_a = 0.5404$$

$$P_3/P_{\text{ob}} = 4.9196$$

$$\begin{aligned} \dot{W}_{\text{driver}} = \dot{W}_a &= 0.0011023 \text{ lbm/s} \div 0.5404 \\ &= 0.00204 \text{ lbm/s} \end{aligned}$$

The choked nozzle flow equation is given by

$$\frac{\dot{W} T_{\text{oa}}^{0.5}}{C_D P_{\text{oa}} A^*} = \left[\frac{\gamma(MW) g_c \left(\frac{2}{\gamma+1} \right)^{\frac{\gamma+1}{\gamma-1}}}{R} \right]^{0.5} \quad (\text{A-3})$$

With

$$\dot{W}_a = 0.00204 \text{ lbm/s},$$

$$T_{\text{oa}} = 1500 \text{ }^\circ\text{R},$$

$$C_D = 0.9,$$

$$P_{\text{oa}} = 0.3 \text{ Torr or } 0.005803 \text{ lbf/in}^2,$$

$$\gamma = 1.67,$$

$$MW = 40,$$

$$g_c = 32.2 \text{ ft lbf/lbm sec}^2,$$

and

$$R = 1545 \text{ ft lbf/lbm }^\circ\text{R},$$

then

$$A^* = A_{\text{driver throat}} = 21.609 \text{ in}^2$$

or

$$D_{\text{driver throat}} = 5.2453 \text{ in.}$$

With

$$AR = A_{\text{mixer}}/A_{\text{driver throat}} = 300,$$

then

$$A_{\text{mixer}} = 6482.6 \text{ in}^2$$

or

$$D_{\text{mixer}} = 7.57 \text{ ft.}$$

Case B

Choose

$$PR = 0.0005,$$

$$AR = 600,$$

and

$$TR = 5,$$

then

$$P_{\text{driver}} = P_{\text{oa}} = 0.6 \text{ Torr}$$

$$T_{\text{driver}} = 1500 \text{ }^\circ\text{R},$$

From Table A-1,

$$\dot{W}_b/\dot{W}_a \text{ (actual)} = 0.617575 \times 0.9 = 0.5558,$$

and

$$P_3/P_{\text{ob}} \text{ (actual)} = 5.51343 \times 0.9 = 4.9621$$

Then,

$$\dot{W}_{\text{driver}} = \dot{W}_a = \frac{0.0011023 \text{ lbm/s}}{0.5558} = 0.0019833 \text{ lbm/s}$$

$$P_{\text{oa}} = 0.6 \text{ Torr or } 0.011605 \text{ lbf/in}^2.$$

Substituting the values of \dot{W}_a , T_{oa} , C_d , P_{oa} , γ , MW , g_c , and R into the choked nozzle flow equation, we obtained $A_{\text{driver throat}} = 10.505 \text{ in}^2$

and

$$D_{\text{driver throat}} = 3.657 \text{ in.}$$

Since

$$AR = A_{\text{mixer}}/A_{\text{driver throat}} = 600,$$

thus

$$A_{\text{mixer}} = 6303 \text{ in}^2,$$

and

$$D_{\text{mixer}} = 7.46 \text{ ft.}$$

(3.3) Calculations of Driver Nozzle, Mixer, on First Stage Outlet

From Table A-1, for the case of $AR = 600$ and $PR = 0.0005$, we obtain

$$P_1/P_{ob} = P_{\text{nozzle exit}} / P_{\text{suction}} = 0.511492$$

$$P_{\text{nozzle exit}} = P_1 = 0.511492 \times 3 \times 10^{-4} \text{ Torr} = 1.53448 \times 10^{-4} \text{ Torr}$$

$$P_{\text{nozzle exit}}/P_{\text{nozzle inlet}} = P_1/P_{oa}$$

$$= 1.53448 \times 10^{-4}/0.6 = 0.0002557$$

Applying the values of P_1/P_{oa} to a standard isentropic flow table for ideal gas, we obtain

$$M_{\text{nozzle exit}} = 8.91403,$$

$$T_{\text{nozzle exit}} / T_{oa} = 0.036207$$

and

$$A_{\text{nozzle exit}} / A_{\text{driver throat}} = 46.94$$

Then,

$$A_{\text{nozzle exit}} = (10.505)(46.94) \text{ in}^2 = 493.1 \text{ in}^2,$$

$$D_{\text{nozzle exit}} = 3.657 \text{ in} \times (46.94)^{0.5} = 25.05 \text{ in},$$

and

$$T_{\text{nozzle exit}} = (1500 \text{ }^\circ\text{R})(0.036207) = 54 \text{ }^\circ\text{R}$$

$$\dot{W}_t = \text{Total Argon flow rate} = 0.0019833 \text{ lbm/s} + 0.001023 \text{ lbm/s}$$

$$= 0.0030856 \text{ lbm/s}$$

The gas temperature in the mixer, T_{mix} (assuming constant C_p)

$$\begin{aligned} &= (\dot{W}_a T_{nozzle\ exit} + \dot{W}_b T_{ob}) / (\dot{W}_a + \dot{W}_b) \\ &= [0.0019833(54) + 0.0011023(300)] / 0.0038656 \\ &= 142 \text{ }^\circ\text{R} \end{aligned}$$

At the exit of the first stage ejector,

$$\begin{aligned} \dot{W}_t &= 0.0030856 \text{ lbm/s} \\ T &= 142 \text{ }^\circ\text{R} \\ P_3/P_{ob} \text{ (actual)} &= 4.9621 \end{aligned}$$

or

$$\begin{aligned} P_3 &= 4.9621 \times 3 \times 10^{-4} \text{ Torr} \\ &= 1.48863 \times 10^{-3} \text{ Torr} \\ &= 2.8793 \times 10^{-5} \text{ lbf/in}^2 \\ \rho_{exit} &= \frac{P(MW)}{RT} = 7.5595 \times 10^{-7} \text{ lbm/ft}^3 \\ V_{exit} &= \frac{\dot{W}_t}{\rho_{exit}} = 4.08176 \times 10^3 \text{ ft}^3/\text{s} \end{aligned}$$

However, one oil vapor booster pump can only handle a volume flow rate of 776.9 ft³/s, therefore, a second "preboost" stage is required. (Note, ~63 oil vapor pumps are needed in this case).

4. Calculations of a Second Stage Ejector

Utilizing the standard ejector program (Ref. 12), calculations were performed for a second stage ejector with results shown in Table A-2, where

$$\begin{aligned} \dot{W}_b &= \dot{W}_{suction} = 0.0030856 \text{ lbm/s (per port)} \\ P_{ob} &= P_{suction} = 1.48863 \times 10^{-3} \text{ Torr} = 2.8793 \times 10^{-5} \text{ lbf/in}^2 \\ T_{ob} &= 142 \text{ }^\circ\text{R} \end{aligned}$$

Case A

Choose

$$p_2 = \frac{P_{ob}}{P_{oa}} = 0.001,$$

$$PR = \frac{T_{0a}}{T_{0b}} = 10 \quad (T_{0a} = 1500 \text{ } ^\circ\text{R}),$$

and

$$AR = \frac{\dot{V}_{\text{mixer}}}{\dot{V}_{\text{driver throat}}} = 250$$

Then

$$\frac{\dot{W}_b}{\dot{W}_a} \text{ (actual)} = 0.9 \times 0.722947 = 0.65065$$

$$\text{and } \frac{P_3}{P_{0b}} \text{ (actual)} = 0.9 \times 5.93925 = 5.3904$$

Hence

$$\dot{W}_a = \dot{W}_{\text{driver}} = 0.0047423 \text{ lbm/s}$$

and

$$P_{0a} = P_{\text{driver}} = 2.3793 \times 10^{-2} \text{ lbf/in}^2 \text{ (1.48353 Torr)}$$

Substituting the values of T_{0a} , W_a , C_D (0.95), P_{0a} , γ , M , J_c , and R into the choked nozzle flow equation, we obtain

$$A_{\text{driver throat}} = A^* = 10.1245 \text{ in}^2$$

$$D_{\text{driver throat}} = 3.59 \text{ in}$$

therefore,

$$A_{\text{mixer}} = 250 \times 10.1245 = 2532 \text{ in}^2$$

$$D_{\text{mixer}} = 57.39 \text{ in.}$$

Case B

Choose

$$PR = 0.0005,$$

$$AR = 500,$$

and

$$T_{0a} = 1500 \text{ } ^\circ\text{R}$$

then

$$\frac{\dot{W}_B \text{ (actual)}}{\dot{W}_A} = 0.9 \times 0.715497 = 0.64395,$$

$$\dot{W}_A = \dot{W}_{\text{driver}} = 0.0047915 \text{ lbm/s},$$

$$\frac{P_3}{P_{ob}} = \frac{P_{\text{exit}}}{P_{\text{suction}}} = 0.9 \times 6.25347 = 5.62812$$

$$P_{oa} = \frac{P_{ob}}{PR} = \frac{2.8793 \times 10^{-5} \text{ lbf/in}^2}{0.0005} = 0.057586 \text{ lbf/in}^2 \text{ (2.377 Torr)}$$

Substituting the values of T_{oa} , \dot{W}_A , C_D , P_{oa} , γ , MW , g_c and R into the choked nozzle flow equation,

we obtain

$$A_{\text{driver throat}} = 5.11487 \text{ in}^2$$

and

$$D_{\text{driver throat}} = 2.552 \text{ in}$$

Therefore

$$A_{\text{mixer}} = 500 \times 5.11487 \text{ in}^2 = 2557 \text{ in}^2$$

and

$$D_{\text{mixer}} = 57.06 \text{ in.}$$

Results of Cases A and B indicate that changing the pressure ratio of the driver and the suction does not affect the mixer size significantly. Thus, results from Case B were used for further calculations.

Exit Conditions of Nozzle

From Table A-2,

$$P_1/P_{ob} = 0.516362$$

since

$$\frac{P_{ob}}{P_{oa}} = 0.0005,$$

$$P_{ob}$$

$$\therefore \frac{P_1}{P_{oa}} = 0.0005 \times 0.516362 = 0.00025818$$

Applying the results of P_1/P_{oa} to a standard isentropic flow table for ideal gas, we obtain

$$\dot{m}_{\text{nozzle exit}} = 3.9,$$

$$A_{\text{nozzle exit}}/A_{\text{driver throat}} = 46.73,$$

and

$$T_{\text{nozzle exit}}/T_{\text{driver}} = 0.03632$$

then

$$A_{\text{nozzle exit}} = 46.73 \times 5.1149 \text{ in}^2 = 239 \text{ in}^2,$$

$$D_{\text{nozzle exit}} = 17.445 \text{ in},$$

$$T_{\text{nozzle exit}} = 0.03632 \times 1500 \text{ }^\circ\text{R} = 54.5 \text{ }^\circ\text{R}$$

$$\begin{aligned} \dot{m}_t &= \text{total Argon flow rate} \\ &= 0.0030356 + 0.0047916 = 0.0078272 \text{ lbm/s} \end{aligned}$$

T_{mix} = gas temperature in the mixer (assuming constant C_p)

$$\approx = \frac{0.0030356 \times 142 + 0.0047916 \times 54.5}{0.0078272}$$

$$= 91.9 \text{ }^\circ\text{R}$$

From Table A-2,

$$P_3/P_{0b} = 5.62812$$

$\therefore P_3$ = second stage ejector exit pressure

$$= 5.62812 \times 2.8793 \times 10^{-5} \text{ lbf/in}^2$$

$$= 1.6205 \times 10^{-4} \text{ lbf/in}^2 \text{ (3.3781} \times 10^{-3} \text{ Torr)}$$

$$\rho_{\text{exit}} = \frac{P_3 \text{ (MW)}}{RT_{\text{mix}}} = 6.57397 \times 10^{-6} \text{ lbm/ft}^3$$

$$\dot{V}_{\text{exit}} = \dot{m}_t/\rho_{\text{exit}} = 1193.2 \text{ ft}^3/\text{s (per port)}$$

However, one oil vapor booster pump can only handle a volume flow rate of 776.9 ft³/s, and, therefore, a third "preboost" stage is needed. (NOTE: We now need 13 oil vapor booster pumps instead of 12).

5. Calculations of a Third Stage Ejector

Results of a third stage ejector performances calculated by the standard ejector program (Ref. 12) are listed in Table A-3, where

$$\dot{W}_b = \dot{W}_{\text{suction}} = 0.0078772 \text{ lbm/s (per port)}$$

$$P_{ob} = P_{\text{suction}} = 1.6205 \times 10^{-4} \text{ lbf/in}^2 \text{ (0.008379 Torr)}$$

$$T_{ob} = T_{\text{suction}} = 91.9 \text{ }^\circ\text{R}$$

Choose

$$PR = P_{ob}/P_{oa} = 0.001$$

$$TR = T_{oa}/T_{ob} = 16 \text{ (} T_{oa} = 1500 \text{ }^\circ\text{R)}$$

$$AR = A_{\text{mixer}} / A_{\text{driver throat}} = 300$$

From Table A-3,

$$\dot{W}_b/\dot{W}_a \text{ (actual)} = 0.9 \times 1.07407 = 0.96666$$

and

$$P_3/P_{ob} \text{ (actual)} = 0.9 \times 5.05017 = 4.54515$$

Thus

$$\dot{W}_a = \dot{W}_{\text{driver}} = \dot{W}_b/0.96666 = 0.0081489 \text{ lbm/s}$$

$$P_{oa} = P_{\text{driver}} = P_{ob}/0.001 = 0.16205 \text{ lbf/in (8.38 Torr)}$$

Assuming $C_D = 0.95$ and substituting the values of T_{oa} , \dot{W}_a , C_D , P_{oa} , γ , MW , g_c , and R into the choked nozzle flow equation, we obtain

$$A_{\text{driver throat}} = A^* = 3.09115 \text{ in}^2$$

$$D_{\text{driver throat}} = 1.9839 \text{ in.}$$

Therefore

$$A_{\text{mixer}} = 300 \times 3.09115 \text{ in}^2 = 927 \text{ in}^2$$

and

$$D_{\text{mixer}} = 34.36 \text{ in.}$$

Exit Conditions of Nozzle

From Table A-3,

$$P_1/P_{ob} = 0.519373,$$

Since

$$P_{ob}/P_{oa} = 0.001$$

$$\therefore P_1/P_{oa} = 0.0005194$$

Applying the results of P_1/P_{0a} to a standard isentropic flow table for ideal gas, we obtain

$$M_{\text{nozzle exit}} = 7.6848,$$

$$T_{\text{nozzle exit}} / T_{0a} = 0.048114,$$

and

$$A_{\text{nozzle exit}} / A_{\text{driver throat}} = 30.901$$

Then

$$A_{\text{nozzle exit}} = 30.901 \times 3.09115 \text{ in}^2 = 95.52 \text{ in}^2$$

$$D_{\text{nozzle exit}} = 11.028 \text{ in}$$

$$T_{\text{nozzle exit}} = 0.048114 \times 1500 \text{ }^\circ\text{R} = 72 \text{ }^\circ\text{R}$$

$$\dot{W}_t = \text{total Argon flow rate}$$

$$= 0.0078772 + 0.0081489 = 0.016026 \text{ lbm/s}$$

$$T_{\text{mix}} = \text{gas temperature in mixer (assuming constant } C_p)$$

$$= \frac{0.0078722 \times 91.9 + 0.0081489 \times 72}{0.016026}$$

$$= 81.9 \text{ }^\circ\text{R}$$

From Table A-3,

$$P_3/P_{0b} = 4.54515$$

$$P_3 = \text{third stage ejector exit pressure}$$

$$= 4.54515 \times 1.6205 \times 10^{-4} \text{ lbf/in}^2$$

$$= 8.9859 \times 10^{-4} \text{ lbf/in}^2 \text{ (0.04646 Torr)}$$

$$c_{\text{exit}} = \frac{P_3 \text{ (MW)}}{RT_{\text{mix}}} = 4.0905 \times 10^{-5} \text{ lbm/ft}^3$$

$$\dot{V}_{\text{exit per port}} = \dot{W}_t / c_{\text{exit}} = 391.8 \text{ ft}^3/\text{s}$$

The results of D_{mix} of 34.36 in and \dot{V}_{exit} of 391.8 ft³/s are within the design range of pump inlet diameter of 36 in and volume flow rate of 776.9 ft³/s.

6. Calculations of Roots Mechanical Blowers Requirement

The oil vapor booster pumps can discharge against a back pressure of > 3 Torr, whereas, the third stage Argon ejector needs 9 Torr. Thus, a roots type mechanical blower is needed to boost from 2 to 50 Torr.

At

$$P_1 = 2 \text{ Torr (0.038684 lbf/in}^2\text{)}$$

$$T = 530 \text{ }^\circ\text{R}$$

$$\dot{W} = 0.016026 \text{ lbm/s (per port)}$$

then

$$\rho = 2.72114 \times 10^{-4} \text{ lbm/ft}^3$$

and

$$\dot{V} = \dot{W}/\rho = 58.89 \text{ ft}^3/\text{s or } 3534 \text{ ft}^3/\text{min (per port)}$$

HP = horse power of the roots blower

$$= \left(\frac{\gamma}{\gamma-1} \right) P_1 V_1 \left[\left(\frac{P_2}{P_1} \right)^{(\gamma-1)/\gamma} - 1 \right]$$

with

$$P_2/P_1 = 50/2 = 25.$$

The horse power required assuming an efficiency of 70% is

$$= \frac{1.67}{(1.67-1)} \times \frac{0.038684 \text{ lbf/in}^2}{0.7} \times \frac{3534 \text{ ft}^3/\text{min} \times 144 \text{ in}^2/\text{ft}^2}{33000 \text{ ft-lbf/hp min}} (25^{0.4012} - 1)$$

$$= 5.6 \text{ hp per port.}$$

The required horse power for the roots blower is small.

Table A-1

RESULTS FOR THE FIRST STAGE EJECTOR OPTIMIZATION PROGRAM

Press Ratio is .001 Gamma A is 1.67 Gamma B is 1.67
 Temp Ratio is 5 Mol Wt Ratio is 1

Area Ratio	P1/Pob	Wb/Wa	P3/Pob
200	.535545	.377528	7.75368
220	.531129	.422055	7.12957
240	.527452	.466616	6.6096
260	.524343	.511201	6.16972
280	.52168	.555806	5.7928
300	.519373	.600426	5.46617
320	.517355	.64506	5.18046

Press Ratio is .0005 Gamma A is 1.67 Gamma B is 1.67
 Temp Ratio is 5 Mol Wt Ratio is 1

Area Ratio	P1/Pob	Wb/Wa	P3/Pob
400	.523678	.394371	7.82323
420	.521935	.416674	7.49314
440	.520351	.438983	7.19306
460	.518906	.461295	6.91912
480	.517581	.483612	6.668
500	.516362	.505933	6.43705
520	.515238	.528256	6.22386
540	.514196	.550583	6.02647
560	.513231	.572911	5.84322
580	.512331	.595243	5.6726
600	.511492	.617575	5.51343

Table A-2

RESULTS FOR THE SECOND STAGE EJECTOR OPTIMIZATION PROGRAM

Press Ratio is .001 Gamma A is 1.67 Gamma B is 1.67
 Temp Ratio is 10 Mol Wt Ratio is 1

Area Ratio	P1/Pob	Wb/Wa	P3/Pob
100	.584432	.220732	14.4851
150	.551753	.376801	9.88355
200	.535545	.533905	7.5827
220	.531129	.596876	6.95507
240	.527452	.659894	6.43194
260	.524343	.722947	5.98928

Press Ratio is .0005 Gamma A is 1.67 Gamma B is 1.67
 Temp Ratio is 10 Mol Wt Ratio is 1

Area Ratio	P1/Pob	Wb/Wa	P3/Pob
200	.56031	.243224	14.6078
250	.545688	.321587	11.8232
300	.535894	.400184	9.96683
320	.532838	.431663	9.38668
340	.530142	.463159	8.87475
360	.527747	.49467	8.41972
380	.525604	.526193	8.01261
400	.523678	.557725	7.64616
420	.521935	.589266	7.3146
440	.520352	.620815	7.01317
460	.518906	.65237	6.73791
480	.517581	.683931	6.48562
500	.516362	.715497	6.25347

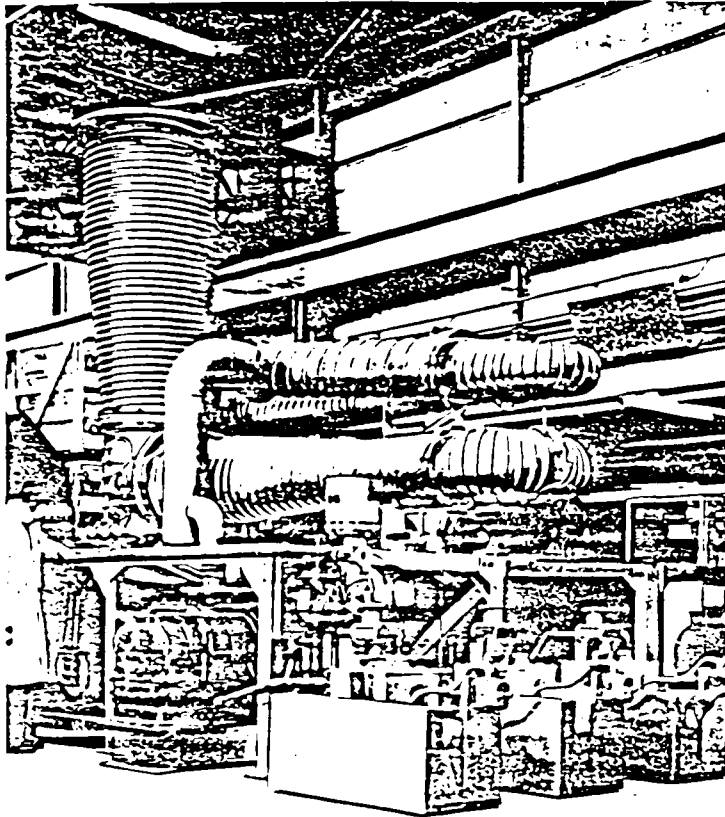
Table A-3

RESULTS FOR THE THIRD STAGE EJECTOR OPTIMIZATION PROGRAM

Press Ratio is .001 Gamma A is 1.67 Gamma B is 1.67
Temp Ratio is 16 Mol Wt Ratio is 1

Area Ratio	P1/Pob	Wb/Wa	P3/Pob
200	.535545	.675342	7.39659
250	.525835	.874581	5.99626
300	.519373	1.07407	5.05017

Oil vapour booster pumps—22000 l s⁻¹



Model 100B4	
Pumping speed (air)	22000 l s ⁻¹
Ultimate vacuum	10 ⁻⁴ torr
Critical backing pressure	1.2 to 1.5 torr
Recommended backing pump displacement for maximum throughput	3600 m ³ h ⁻¹
Recommended backing pumps	ER2000 + ER600 + ES4000
Fluid capacity	320 litre
Heater loading (maximum)	90kW
Warming-up time for full performance at max heater input	60 min
Minimum water flow	7200 l h ⁻¹
Water connexion	1½ in BSP
Weight	3090kg
Product description	
Pump 340-380V 3 ph 50/60Hz star	05-B067-01-380
400-440V 3 ph 50/60Hz star	05-B067-01-440
Spares	
Kit comprising seals, fuses, etc.	14-B067-01-801
Heater (Tubaiox bank type) — state voltages	Dev 1512-10A
Fluid AP201 20 litre	09-H026-01-052
Accessories 36 in (914mm) system	
Model P36R36 pneumatically operated right-angled isolation valve	05-B054-00-000
Model CB36 water cooled chevron battle	06-B055-06-000

Refer to vapour pump accessories section for complete data on accessories.

For full range of vapour pump fluids, see fluids and sealants section.

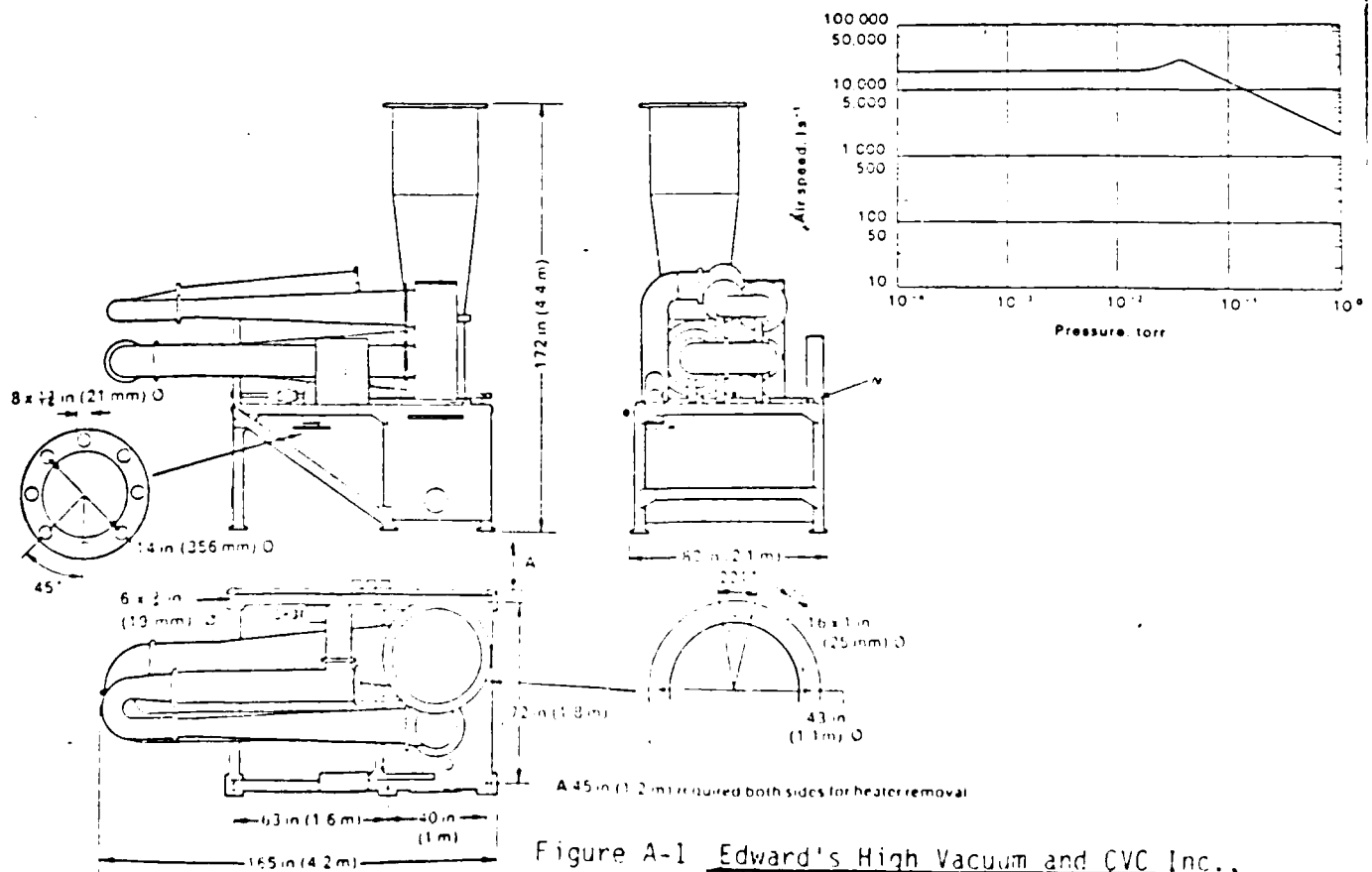


Figure A-1 Edward's High Vacuum and CVC Inc., Oil Vapor Booster Pumps

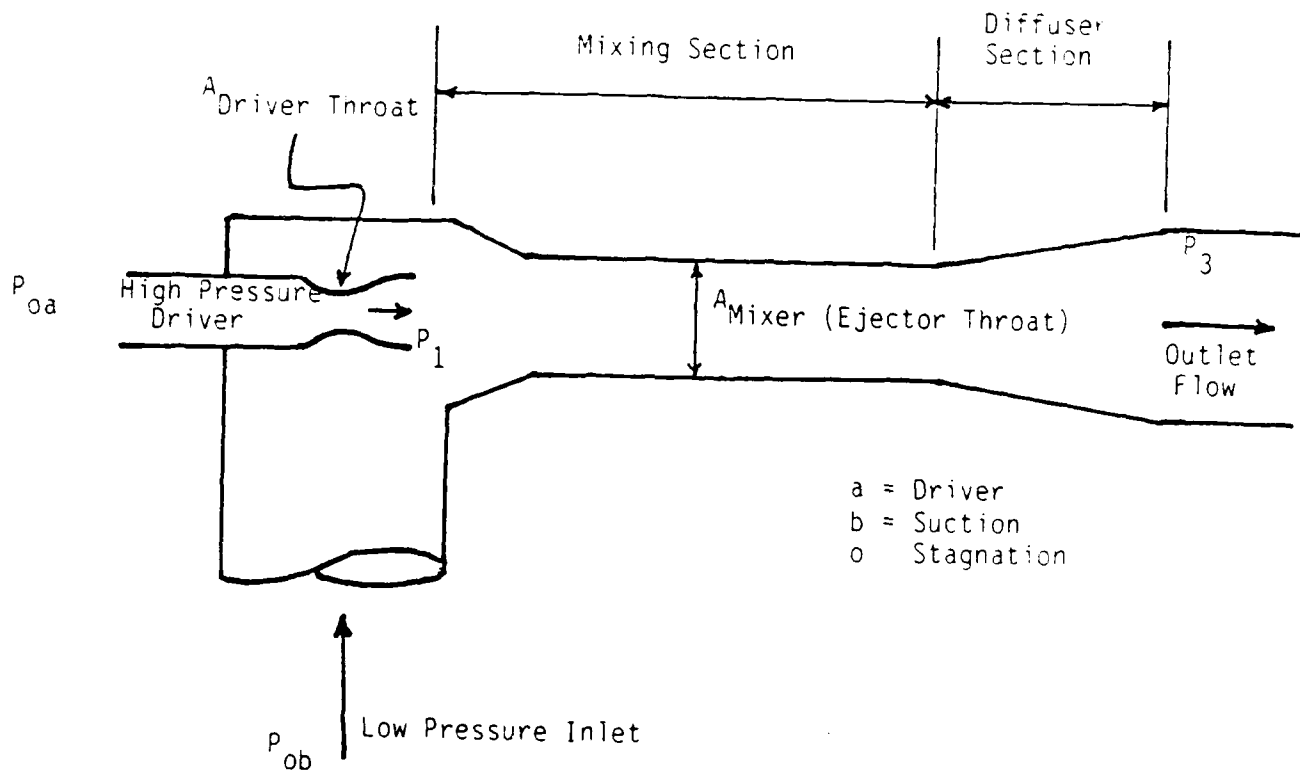


Figure A-2 A Schematic of an Ejector Prebooster System

END
DATE
FILMED
DTIC
4/88

END
DATE
FILMED
DTIC
4/88